applied sciences

MDPI

Review

Soliton Molecules and Multisoliton States in Ultrafast Fibre Lasers: Intrinsic Complexes in Dissipative Systems

Lili Gui [1,*], Pan Wang [2], Yihang Ding [2], Kangjun Zhao [2], Chengying Bao [3], Xiaosheng Xiao [2] and Changxi Yang [2,*]

1 4th Physics Institute and Research Center SCoPE, University of Stuttgart, Pfaffenwaldring 57, 70569 Stuttgart, Germany

2 State Key Laboratory of Precision Measurement Technology and Instruments, Department of Precision Instruments, Tsinghua University, Beijing 100084, China; p-wang14@mails.tsinghua.edu.cn (P.W.); dingyh17@mails.tsinghua.edu.cn (Y.D.); zhaokj16@mails.tsinghua.edu.cn (K.Z.); xsxiao@tsinghua.edu.cn (X.X.)

3 Watson Laboratory of Applied Physics, California Institute of Technology, Pasadena, CA 91125, USA; cbao@caltech.edu

* Correspondence: l.gui@pi4.uni-stuttgart.de (L.G.); cxyang@tsinghua.edu.cn (C.Y.); Tel.: +86-10-6277-2824 (C.Y.)

Received: 14 December 2017; Accepted: 23 January 2018; Published: 29 January 2018

Featured Application: High-capacity telecommunication, advanced time-resolved spectroscopy, self-organization and chaos in dissipative systems.

Abstract: Benefiting from ultrafast temporal resolution, broadband spectral bandwidth, as well as high peak power, passively mode-locked fibre lasers have attracted growing interest and exhibited great potential from fundamental sciences to industrial and military applications. As a nonlinear system containing complex interactions from gain, loss, nonlinearity, dispersion, etc., ultrafast fibre lasers deliver not only conventional single soliton but also soliton bunching with different types. In analogy to molecules consisting of several atoms in chemistry, soliton molecules (in other words, bound solitons) in fibre lasers are of vital importance for in-depth understanding of the nonlinear interaction mechanism and further exploration for high-capacity fibre-optic communications. In this Review, we summarize the state-of-the-art advances on soliton molecules in ultrafast fibre lasers. A variety of soliton molecules with different numbers of soliton, phase-differences and pulse separations were experimentally observed owing to the flexibility of parameters such as mode-locking techniques and dispersion control. Numerical simulations clearly unravel how different nonlinear interactions contribute to formation of soliton molecules. Analysis of the stability and the underlying physical mechanisms of bound solitons bring important insights to this field. For a complete view of nonlinear optical phenomena in fibre lasers, other dissipative states such as vibrating soliton pairs, soliton rains, rogue waves and coexisting dissipative solitons are also discussed. With development of advanced real-time detection techniques, the internal motion of different pulsing states is anticipated to be characterized, rendering fibre lasers a versatile platform for nonlinear complex dynamics and various practical applications.

Keywords: soliton molecules; bound states; fibre lasers; nonlinear interaction; ultrafast nonlinear optics; fibre optics

1. Introduction

Passively mode-locked fibre lasers generate ultrashort pulses with high peak power and broad optical spectrum, which have attracted growing attention in the past decades due to the advantages of compactness, stability, easy handling and portability [1,2]. The great potential has enabled a wealth of applications in military, industry, fundamental science, biomedicine, etc. In most cases, one single pulse travels through the entire round trip, with a repetition rate inversely proportional to the optical length of the laser cavity. However, higher pumping can lead to pulse splitting and coexistence of several pulses inside the cavity because a fibre laser can only withstand a certain amount of nonlinear phase shift. Depending on a comprehensive interaction via nonlinearity, dispersion, gain, loss, etc. inside the cavity, a fibre laser serves as a complex dissipative system and a versatile platform for plentiful pulse states such as harmonic mode-locking, pulse bunching and soliton molecules [3]. In particular, recent advances on saturable absorbers and dispersion schemes are of important benefit to control the experimental parameters and therefore enable observation of various states of soliton molecules. In analogy to molecules in chemistry which achieve balance of atoms via strong chemical bond, soliton molecules as a boundary soliton state are comprised of several individual pulses and result from balance of repulsive and attraction forces between solitons caused by many effects including nonlinear [for instance, cross phase modulation (XPM), gain saturation, saturable absorption, etc.] and dispersive effects [4]. Such a balance causes that several identical pulses (exactly the same intensity, as well as the same spectral and temporal profiles) travel through the cavity and keep a constant temporal separation and a fixed phase difference between neighbouring pulses. Although solitons pairs exhibiting variant characteristic parameters such as evolving phase [5] are sometimes referred to soliton molecules too, we focus on "soliton molecules" in this Review as stationary soliton pairs preserving all details for at least thousands of round trips in a cavity. Such soliton molecules are of vital significance to understand and explore. The reason is twofold: on the one hand, they are the most frequently observed in fibre lasers as an outcome of the complex nonlinear dynamics, which help us to retrieve the underlying dissipation nature; on the other hand, they are particularly useful for developing larger telecommunication capacity in optical fibre transmission lines [6–8] and advancing ultrafast characterization approaches such as real-time spectroscopy [9,10].

Soliton molecules were first predicted theoretically by Malomed within the framework of nonlinear Schrödinger-Ginzburg-Landau equation [11] and coupled nonlinear Schrödinger equations [12]. Afanasjev et al. and Akhmediev et al. also investigated analytically and numerically the existence and stability of bound states with π, 0 and $\pm\pi/2$ phase differences [13–15]. So far bound states have been studied by simulated and/or experimental methods in types of fibre laser cavities, i.e., in soliton [16,17], stretched-pulse [18], gain-guided [19] and self-similar [20] regimes, as well as dissipative soliton regime associating with large net-normal dispersion and spectral filtering [21]. A lot of experimental observations of bound solitons have been reported in fibre lasers mode-locked by nonlinear polarization evolution (NPE) [22–24], nonlinear amplifying loop mirror (NALM) [8,25] and some real saturable absorbers (e.g., semiconductor saturable absorber mirror (SESAM) [26], carbon nanotubes (CNT) [27–29], graphene [30,31], topological insulator [32], molybdenum disulphide (MoS_2) [33] and black phosphorus [34]). Although a lot of experimental findings have been made in many different cavities, in-phase two-soliton bound states and a systematic observation of soliton molecules with different phase differences were only reported several years ago [28], due to large degree of freedom of manipulation on the experimental configurations in a fibre laser using a real saturable absorber. Later, the rapid development of sorts of mode-lockers promotes discovery and research on bound states and enables complete collection of the stable solutions with π, 0 and $\pm\pi/2$ phase differences predicted in theory.

In this review, we will summarize the state-of-the-art developments on bound solitons in ultrashort fibre lasers. We mainly concentrate on soliton molecules in both experiment and simulation. We will first derive the analytical expression for characterization of soliton molecules in both frequency and time domain. Second, we summarize typical experimental results of soliton molecules with

distinct temporal separations, phase differences and numbers of solitons that appear in kinds of laser cavities. Third, simulation procedures and corresponding findings are intensively addressed. Fourth, we discuss guides and tricks to generation of various bound states and analyse their stability, with nonlinear interaction mechanisms interpreted. Fifth, we extend the content of multisoliton states to other more sophisticated situations and briefly take several cases (soliton rains, rogue waves and coexisting dissipative solitons) which our group has studied as an example, so that a general picture of possible multisoliton complexes is captured. In the end, we give a short conclusion, involve some unexplored parts and mention possible challenges and promising improvement.

2. Analytical Expression of Soliton Molecules for Optical Characterization in Frequency and Time Domain

2.1. Frequency Domain

2.1.1. Two-Soliton Bound States

We assume that the complex amplitude of slowly-varying envelope of a single soliton in time domain can be described by $f(t)$ and the complex amplitude of its optical spectrum can be described by $F(\nu)$, with ν denoting the frequency difference compared to the central optical frequency. It means that Fourier transform of $f(t)$ corresponds to $F(\nu)$.

Consider a two-soliton bound state with pulse separation of ΔT and phase difference of θ_1, which reads $f(t) + f(t - \Delta T)\exp(j\theta_1)$ in time domain. According to Fourier transform, the spectral amplitude of the bound state is expressed by

$$F(\nu) + F(\nu)\exp(-j2\pi\nu\Delta T)\exp(j\theta_1) = F(\nu)\exp[-j(\pi\nu\Delta T - \frac{\theta_1}{2})]\cdot 2\cos(\pi\nu\Delta T - \frac{\theta_1}{2}) \quad (1)$$

The spectral intensity is therefore proportional to

$$|F(\nu) + F(\nu)\exp(-j2\pi\nu\Delta T)\exp(j\theta_1)|_2 = 2|F(\nu)|_2\cdot[1 + \cos(2\pi\nu\Delta T - \theta_1)] \quad (2)$$

Equation (2) indicates that the bound state manifests itself by a modulated optical spectrum under the envelope of 4 times single-soliton counterpart. The modulation period is $\Delta\nu = 1/\Delta T$ and the modulation depth is 100%. Importantly, the intensity at the centre of the spectrum depends on θ_1, which provides us a rather unique method to characterize the phase difference. As an example, the spectra for π, 0 and $\pm\pi/2$ phase differences are shown in Figure 1a–d respectively (the envelope is normalized).

From Figure 1, we can see that out-of-phase and in-phase bound states have symmetrical spectra with respect to the centre wavelength, while $\pm\pi/2$ phase-difference bound states have asymmetrical spectra. In detail, out-of-phase bound state has a minimum at the centre, while in-phase bound state has a maximum at the centre. For comparison, $-\pi/2$ phase-difference bound state has a second maximum peak on the left side (i.e., blue shift) of the first maximum peak, while $\pi/2$ phase-difference bound state has a second maximum peak on the right side (i.e., red shift) of the first maximum peak. Due to close-to-linear leading and trailing edges of the single-soliton spectrum, the spectral peaks of the $\pm\pi/2$ phase-difference bound states satisfy the approximate relationship when modulation period is relatively small

$$I_k \approx (I_{k-1} + I_{k+1})/2\ (k = 2, 3,...), \quad (3)$$

where I_k denotes the intensity of the kth maximum peak.

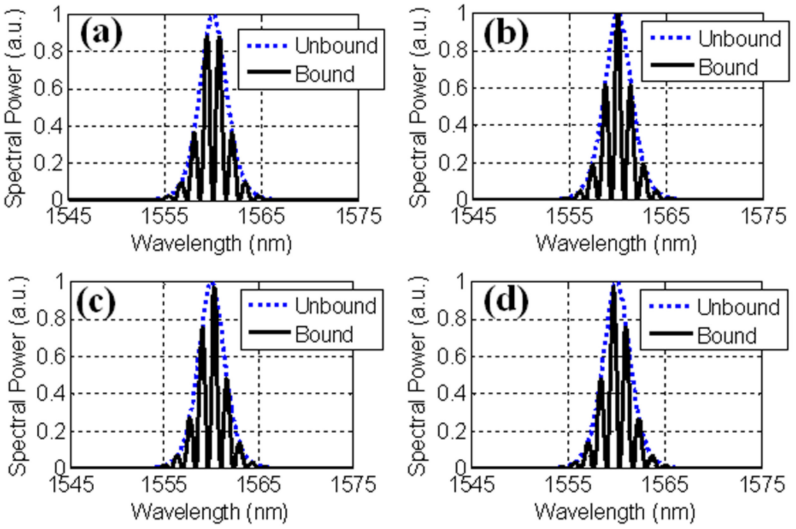

Figure 1. Spectra of two-soliton bound states with θ_1= (**a**) π; (**b**) 0; (**c**) $-\pi/2$; and (**d**) $\pi/2$ according to Equation (2). Blue dotted curve is for single soliton (unbound) and black solid curve is for bound solitons. For all figures, 0.8-ps chirp-free sech-shaped pulses with centre wavelength of 1560 nm and pulse separation of 6 ps are used. (Reproduced with permission from [28]. © The Optical Society of America (Washington, DC, USA), 2013).

2.1.2. Triple-Soliton Bound States

We express a triple-soliton bound state with complex amplitude of solitons in time domain as $f(t)$, $f(t-\Delta T)\exp(j\theta_1)$ and $f(t-2\Delta T)\exp(j\theta_2)$. Then, its spectral amplitude reads

$$\begin{aligned} &F(\nu)+F(\nu)\exp(-j2\pi\nu\Delta T)\exp(j\theta_1)+F(\nu)\exp[-j2\pi\nu\cdot(2\Delta T)]\exp(j\theta_2) \\ &=F(\nu)\exp[-j(2\pi\nu\Delta T-\tfrac{\theta_2}{2})]\cdot\{2\cos(2\pi\nu\Delta T-\tfrac{\theta_2}{2})+\exp[j(\theta_1-\tfrac{\theta_2}{2})]\}. \end{aligned} \tag{4}$$

If $\theta_1=\pi$ and $\theta_2=0$, its spectral intensity is then proportional to

$$\left|F(\nu)\right|_2\cdot[2\cos(2\pi\nu\Delta T)-1]^2=\left|F(\nu)\right|_2\cdot[2\cos(4\pi\nu\Delta T)-4\cos(2\pi\nu\Delta T)+3]. \tag{5}$$

For a guide to eyes, we plot an exemplary optical spectrum of a triple-soliton bound state shown in Figure 2. It exhibits a symmetrical spectrum with respect to the centre wavelength and meanwhile two high peaks are located on both sides of the low central peak.

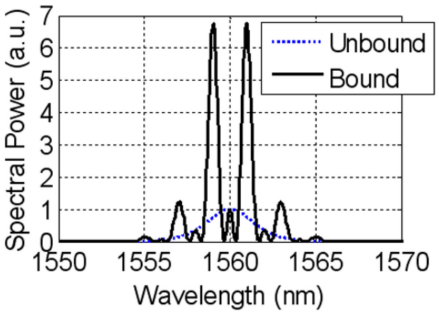

Figure 2. Spectrum of a triple-soliton bound state with $\theta_1=\pi$ and $\theta_2=0$ according to Equation (5). Blue dotted curve is for single soliton (unbound) and black solid curve is for bound solitons. Here 0.8-ps chirp-free sech-shaped pulses with centre wavelength of 1560 nm and pulse separation of 4 ps are employed. (Reproduced with permission from [28]. © The Optical Society of America (Washington, DC, USA), 2013).

2.2. Time Domain

Second-harmonic-generation autocorrelation trace records the intensity autocorrelation function of repetitive ultrashort laser pulses, usually obtained by measuring background-free (noncollinear) second-harmonic generation of nonlinear crystals. It is described by the formula $I_{AC}(\tau) = \int_{-\infty}^{\infty} I(t)I(t-\tau)dt$, where $I(t)$ is the pulse intensity and τ denotes a time delay. In the experiment, the impinging optical pulses are split into two identical beams and then mechanical translation or rotation introduces continuous scan of the time delay of the two beams. The second-harmonic-generation intensity is closely related to the temporal overlap of the two beams. Hence its change with time delay enables us to retrieve the information of the optical pulses in time domain. Autocorrelation trace is the most commonly used measure to characterize the temporal length of an ultrashort optical pulse, by assuming an appropriate temporal profile. Similarly, we can use it for obtaining the temporal details of soliton molecules as complementary information. Figure 3b,c depicts the typical autocorrelation traces of a two- and a triple-soliton molecule respectively, obtained by numerical calculation. For comparison, the autocorrelation trace of the individual soliton atom is illustrated in Figure 3a. For a soliton molecule which is comprised of n identical solitons (only phase might differ), its autocorrelation trace shows $(2n-1)$ peaks and the peak intensity jumps from 1 to n and then back to 1 again step by step. Similar to the situation of conventional single solitons, the width of one individual peak in autocorrelation trace is proportional to the width of one single optical pulse, see Figure 3a,b. Note that autocorrelation trace enables detection of not only temporal separation between adjacent pulses but also the amplitude ratio of them, which are reflected by modulation period and modulation depth in frequency domain. Autocorrelation measurement is not able to reveal the phase relationship between neighbouring solitons, therefore unfortunately less powerful than optical spectrum recording in terms of complete characterization of a soliton molecule.

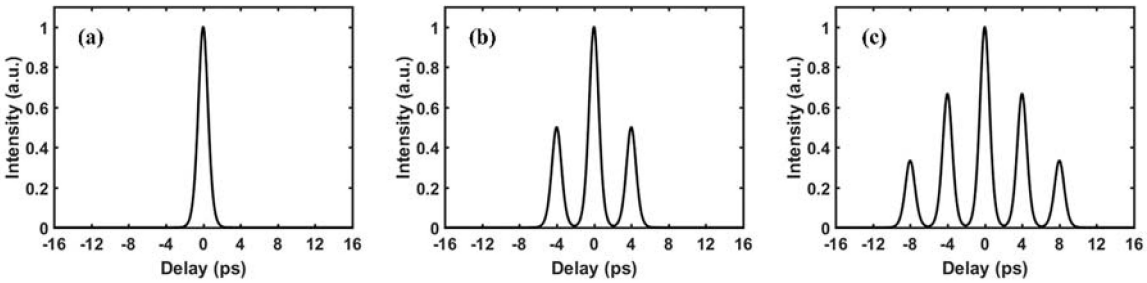

Figure 3. Autocorrelation traces of (**a**) a single soliton; (**b**) a twin-soliton bound state; and (**c**) a triple-soliton bound state. Chirp-free sech-shaped pulses with pulse width of 0.8 ps and temporal distance of 4 ps are utilized.

3. Experimental Observation of Various Soliton Molecules in Different Fibre Lasers

3.1. Anomalous Dispersion Regime

Fibre laser cavities operating in anomalous dispersion regime allow solutions of conventional sech-profiled solitons and have been widely investigated due to the great potential in abundant applications such as fibre optical communications and military security. The typical spectral working bands lie in the range of 1.5 and 2 microns. In this section, main experimental findings on soliton molecules at this spectral window are given, which simultaneously indicate what we have studied in the past several years.

3.1.1. 1.5-Micron Wavelength Regime

Figure 4 shows the laser cavity schematically. A segment of 48-cm long erbium-doped fibre (EDF) is forward pumped by a 980-nm laser diode. The pump laser is coupled into the cavity through a wavelength division multiplexer (WDM). A polarization-independent isolator (PI-ISO) ensures

unidirectional operation of the fibre laser. A polarization controller (PC) is employed to adjust birefringence and optimize operation of the cavity. A polyimide (PI) film incorporating 1 wt. % single-walled carbon nanotubes (SWNT) [35] acts as the saturable absorber (SA), which is inserted between PC and an output coupler. Ninety percent of the laser power is fed back into the cavity to maintain sufficient gain, while 10% output is detected to investigate the generated soliton states. An optical spectrum analyser with 0.06-nm resolution bandwidth, a 2-GHz oscilloscope and a 13.6-GHz radio-frequency (RF) signal analyser with a 2-GHz photo-detector and a second-harmonic-generation autocorrelator are used to characterize the output pulses in detail. The ring cavity is approximately 13 m in length and the net anomalous group-velocity dispersion (GVD) is ~-0.28 ps^2.

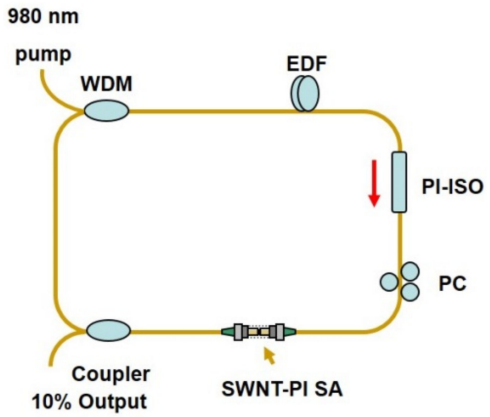

Figure 4. Schematic figure of the laser cavity. WDM: wavelength division multiplexer; EDF: erbium-doped fibre;PI-ISO: polarization-independent isolator; PC: polarization controller; SWNT: single-walled carbon nanotube; PI: polyimide; SA: saturable absorber. (Reproduced with permission from [28]. © The Optical Society of America (Washington, DC, USA), 2013).

1. Two-soliton bound states

Sufficient pump power ensures gain for stable operation of multi-soliton states within the cavity. When polarization state is adjusted by rotating PC orientation carefully, kinds of bound states with different phase differences could be observed. Figure 5a,b shows optical spectrum and autocorrelation trace for an example of soliton molecules with π phase difference. The experimental result (black solid curve of Figure 5a) agrees well with fitting result (red dashed curve of Figure 5a) of bound solitons comprising two sech-profiled pulses with opposite phases. Some imperfection arises from coexistence of continuous-wave (cw) component, generation of sidebands and a little asymmetry of the spectrum. The first two factors are common in a soliton-type fibre laser. The last one is caused mainly by asymmetry of gain spectrum of the erbium fibre and by the third-order dispersion. Modulation period of 2.7 nm and ~100% modulation depth in the experimental spectrum imply that two solitons with 2.8 ps pulse separation have an excellent coherence. Autocorrelation trace (Figure 5b) confirms the temporal distance further, as well as exactly the same pulse width and amplitude of the two bound solitons.

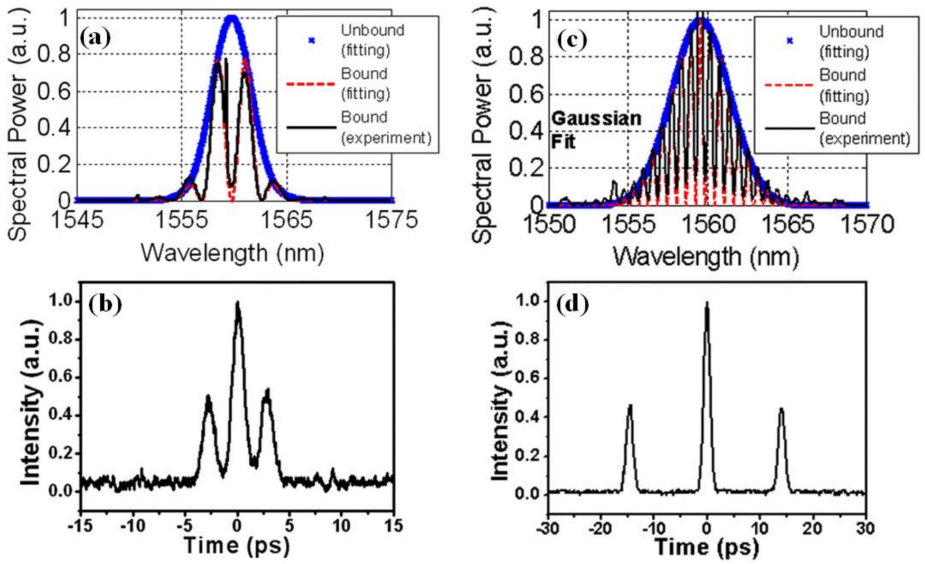

Figure 5. (**a**) The optical spectrum and (**b**) autocorrelation trace of an out-of-phase two-soliton bound state; (**c**) The optical spectrum and (**d**) autocorrelation trace of an in-phase two-soliton bound state. (Reproduced with permission from [28]. © The Optical Society of America (Washington, DC, USA), 2013).

Figure 5c,d shows another example for in-phase bound solitons. The black solid curve of Figure 5c is the experimental optical spectrum with modulation period of 0.6 nm. It can be seen that there is a large cw component existing at the centre of the spectrum and Kelly sidebands observable at trailing edges, which result in slightly imperfect agreement between measurement and fitting by assuming Gaussian-shaped pulses (red dashed). We emphasize that it does not influence the conclusion that the two bound solitons are in phase. Modulation depth of the experimental spectrum seems to be lower than 100%, which is just because a relatively coarse resolution bandwidth (0.2 nm) was used (an optical spectrum analyser is sufficient to resolve the spectrum of a bound state only when modulation period is at least 4 to 5 times the resolution bandwidth [31]). Figure 5d plots the autocorrelation of the bound solitons, indicating pulse full-width at half-maximum (FWHM) of 0.9 ps and pulse separation of 13.5 ps. The pulse separation is the same as that calculated through modulation period of the optical spectrum.

In addition, $\pm\pi/2$ phase-difference bound states were obtained in this laser cavity, as shown by the spectra in Figure 6. Both Figure 6a,b have a prominent asymmetry, which indicates that their phase differences are neither π nor 0. The excellent fitting with sech-shaped pulses concludes the phase differences in both figures, despite of a large cw component coinciding with the maximum peak in Figure 6b.

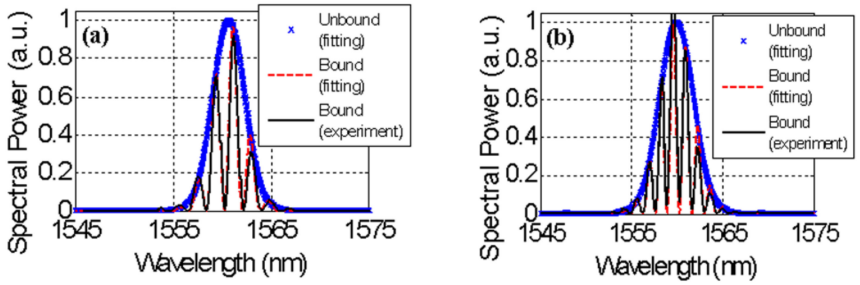

Figure 6. (**a**) Experimental and fitting spectra of a -$\pi/2$ phase-difference two-soliton bound state; (**b**) Experimental and fitting spectra of a $\pi/2$ phase-difference two-soliton bound state. Fitting spectra of the envelope (unbound) are also presented. (Reproduced with permission from [28]. © The Optical Society of America (Washington, DC, USA), 2013).

2. Triple-soliton bound states

According to soliton energy quantization, higher pumping levels can correspond to more numbers of pulses affordable in the cavity. Under appropriate pump power and PC orientation, triple-soliton bound states can be observed experimentally owing to a balance between repulsive and attractive forces. Figure 7 is the optical spectrum of such a state as an example. The spectral shape is very modulated and symmetrical with respect to the centre wavelength and can be nicely fitted by using the analytical expression of a triple-soliton molecule in Equation (4) (fitted parameters are given in the inset).

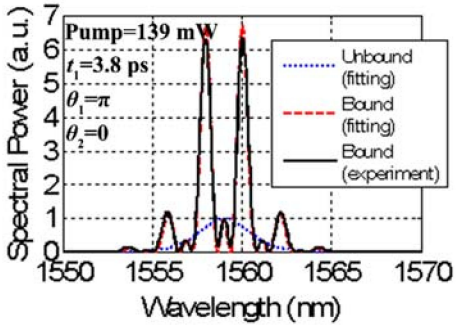

Figure 7. Optical spectrum of a triple-soliton bound state obtained in the laser cavity shown in Figure 4. Black solid curve is for experimental spectrum, red solid curve is for fitting spectrum with parameters marked in the figure and blue dashed curve is for fitting spectrum of a single soliton (unbound). (Reproduced with permission from [28]. © The Optical Society of America (Washington, DC, USA), 2013).

3. Widely spaced bound states

The above-mentioned experimental observations prove existence of tightly bound soliton molecules in fibre lasers, in which the constant and fixed phase relationship is clearly evidenced by the fully modulated spectral fringes. They are ones of the most common examples since the ratio of pulse separation to pulse width (RSW) ranges from a few to a few tens, typical for optical Kerr effect and Raman effects that dominate if two pulses are partially overlapped. In comparison to the strong and short-range mutual interaction between neighbouring solitons, weak and long-range interaction mediated by continuous wave could lead to less bound soliton molecules, which is much more widely spaced. Typically, the temporal separations of such distant multiple solitons can be as large as 100 times pulse durations. Figure 8 exhibits the optical spectra and autocorrelation traces of several examples. The laser cavity to generate those widely spaced bound solitons is very similar to that in Figure 4 [31]. Differently, multilayer graphene with modulation depth of 6% and insertion loss of 2.5 dB is utilized as the saturable absorber. Output coupling ratio is also tailored in order to control the nonsoliton intensity and measure the autocorrelation traces.

As we can see from the optical spectra in Figure 8, the intensity of the continuous-wave component is usually very gigantic in the situations of widely spaced bound solitons, indicating the important role of nonsoliton component in the generation of loosely bound states. In most cases, loosely bound states were produced from states of two-pulse bunches with small separation assisted by nonsoliton components. In the state of two-pulse bunches, energy of nonsoliton components can range from several to tens of percent soliton energy. The residual continuous wave in the cavity works as efficient medium to balance solitons with temporal separation of two orders of magnitude of pulse width. Although this sort of long-range interaction is relatively weak, it is capable of connecting the distant pulses very coherently, namely, preserving the phase-locked situation for a large number of round trips (note that the modulation depth less than 100% in Figure 8 is due to the coarse resolution of the spectrometer [31], rather than a relaxed nature of the soliton pairs).

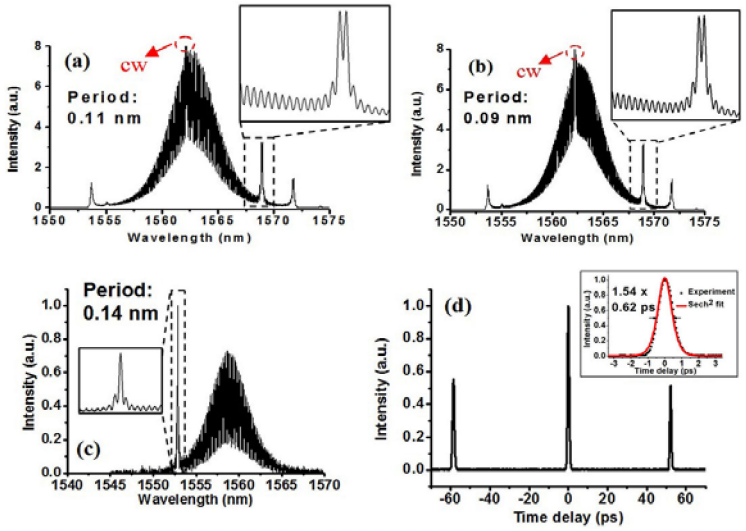

Figure 8. (**a**–**c**) Optical spectra of different loosely bound states (insets: partial magnification); (**a**,**b**) 90/10 coupler; (**c**) 50/50 coupler; (**d**) Autocorrelation trace in correspondence with the bound state in (**c**). Inset is magnified view of the central peak fitted by sech^2 profile. (© 2013 IEEE, Piscataway, NJ, USA. Reprinted, with permission from [31]).

3.1.2. 2-Micron Wavelength Regime

Standard silica-based optical fibres generally feature a large anomalous chromatic dispersion at a wavelength around 2 µm, so that passively mode-locked thulium (Tm) fibre lasers usually operate in large net anomalous dispersion regime. Combined with intense pumping, this situation is conducive to multiple pulsing at 2 µm such as noise-like pulse generation [36], pulse bunching [37], soliton rains [38], harmonic mode locking [39] and soliton molecules [23,24,40].

A Tm fibre laser based on NPE mode-locking technique is shown in Figure 9. The laser is backward pumped by a 1550 nm laser diode (LD) seeded erbium-doped fibre amplifier (EDFA). Two PCs and a polarization-dependent isolator (PD-ISO) are utilized for NPE mode-locking. 2.3-m-long thulium-holmium-doped silica fibre (TDF) is used as active fibre. The total cavity length is 4.7 m, with net dispersion of -0.329 ps^2. The 50/50 output is monitored by an optical spectrum analyser, a second-harmonic autocorrelator, a 2 GHz oscilloscope via a 1 GHz photodetector and an RF signal analyser.

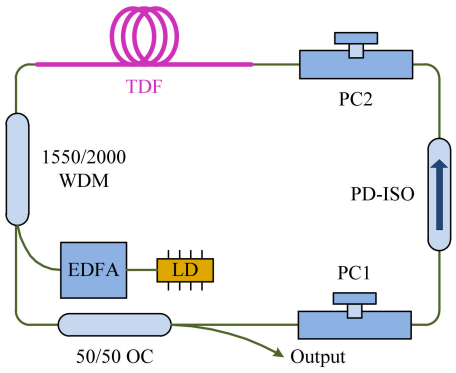

Figure 9. Scheme of the NPE-based mode-locked thulium-holmium co-doped fibre laser; LD: laser diode; EDFA: erbium-doped fibre amplifier; WDM: wavelength division multiplexer; TDF: thulium-holmium-doped fibre; PC: polarization controller; PD-ISO: polarization-dependent isolator; OC: optical coupler. (Reproduced with permission from [23]. © The Optical Society of America (Washington, DC, USA), 2016).

Under appropriate cavity parameters, stable soliton molecules are obtained, as shown in Figure 10. The optical spectrum, in conjunction with the optical autocorrelation trace, demonstrates phase locking of the two bound solitons. The symmetric structure of the spectrum with a central dip indicates that the soliton pairs are out of phase. The autocorrelation trace has three peaks with the intensity ratio of 1:2:1 and the same width, implying that the two bound solitons have the same intensity, pulse duration and a constant separation. The oscilloscope trace as well as the RF spectrum confirm again high stability.

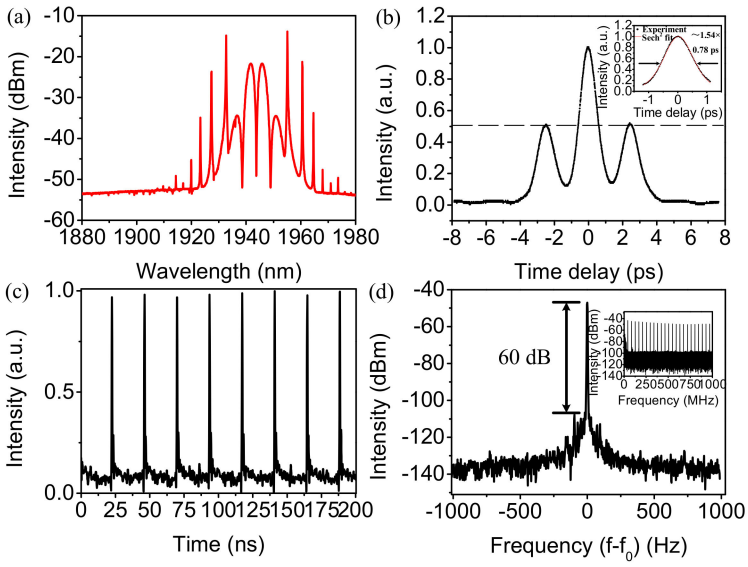

Figure 10. Experimental observation of a stationary soliton pair at ~1940 nm: (**a**) optical spectrum; (**b**) optical autocorrelation trace (inset: magnified view of the central peak fitted by sech^2 profile); (**c**) pulse train on oscilloscope; (**d**) radio-frequency (RF) spectrum (inset: RF spectrum over a 1-GHz span). (Reproduced with permission from [23]. © The Optical Society of America (Washington, DC, USA), 2016).

3.2. Net Normal Dispersion Regime

Ortaç et al. studied an ytterbium-doped fibre laser operating in net normal dispersion regime [20]. The cavity is designed carefully with total cavity GVD of +0.047 ps^2 such that the pulses are always positively chirped when propagating along the whole cavity and are shortest in pulse duration near the beginning of the fibre just after the intra-cavity grating pairs. A self-similar propagation of the pulses inside the cavity can then be guaranteed. By intentionally choosing the orientation of the intra-cavity polarization controllers they were able to observe bound states of two and three parabolic pulses in a self-similar regime, for the first time. Figure 11a,b shows the optical spectrum and corresponding autocorrelation trace of one two-pulse bound state, which confirm generation of parabolic pulses by fitting them with different profiled functions.

By tailoring dispersion condition of a fibre laser and especially controlling spectral filtering bandwidth, gain-guided solitary pulses can be formed [41,42]. Different from self-similar evolution which generates linear-chirp parabolic pulses [43], gain-guided fibre lasers are capable of producing pulses with nonlinear frequency chirp. Despite of different pulsing dynamics, bound states of gain-guided solitary pulses have also been observed by Zhao et al. [19], featuring periodic modulation of optical spectrum under envelope with steep borders and relatively flat top, as shown in Figure 12a. The ratio between the measured pulse separation and the pulse width is 34.4 (Figure 12b), which goes far beyond the usual direct pulse-pulse interaction between solitons. By conducting numerical simulations, the authors have nicely revealed interesting properties of such bound solitons that both pulse separation and relative phase difference remain fixed along the entire cavity, although strong

stretching and compression of one individual soliton take place when it propagates inside the laser. Simulation results indicate that at the position where the pulse is longest, partial overlap of the temporal profile of the two bound solitons is present, enabling a direct strong interaction between two pulses.

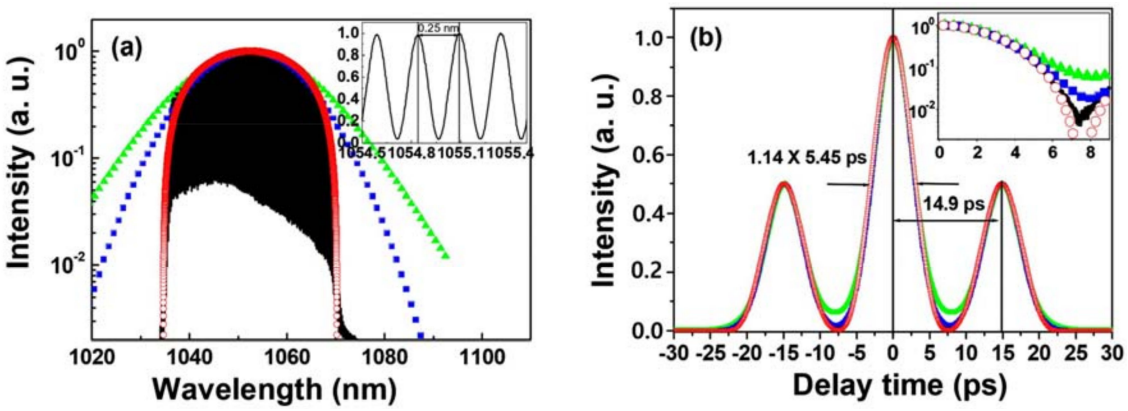

Figure 11. (**a**) Optical spectrum of the soliton molecules. The spectrum is fit with parabolic (open circles), Gaussian (closed squares) and sech^2 (closed triangles) pulse shapes. The inset shows a zoomed-in portion of the optical spectrum on a linear scale illustrating the modulation period; (**b**) Second-order intensity autocorrelation trace of the two bound parabolic pulses observed directly at the laser output. Theoretical fits with parabolic (open circles), Gaussian (closed squares) and sech^2 (closed triangles) profiles are also shown. Inset shows detail of the autocorrelation trace on a logarithmic scale. (Reproduced with permission from [20]. © The Optical Society of America (Washington, DC, USA), 2006).

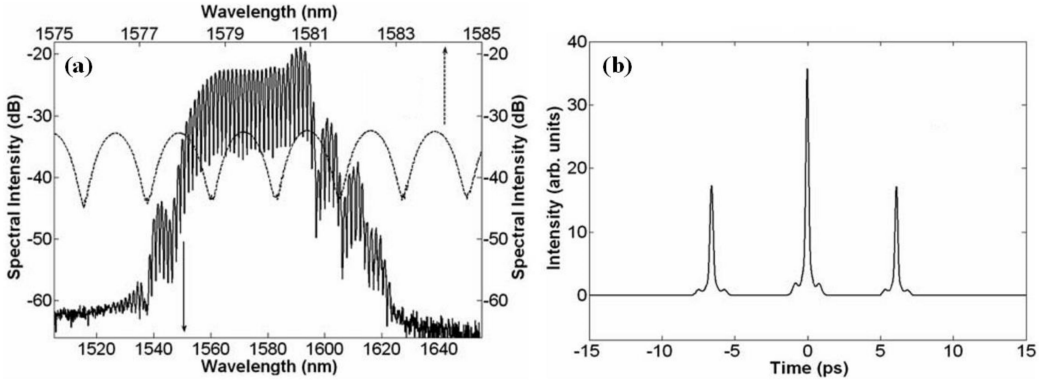

Figure 12. (**a**) Optical spectrum and (**b**) autocorrelation trace of a bound state of gain-guided solitons. (Reproduced with permission from [19]. © The Optical Society of America (Washington, DC, USA), 2007).

3.3. Nearly Zero Net-Cavity Dispersion Regime

A dispersion-managed fibre laser is characterized by segments with dispersion of opposite signs and a very small anomalous or normal net-cavity dispersion is caused. The dispersion management effect ensures large breathing of the pulse width along the cavity. Such nearly zero net-cavity dispersion regime allows existence of Gaussian pulses which are more tolerant with nonlinear phase shift compared to traditional sech-profiled solitons in anomalous dispersion fibre lasers. As some of the pioneers who study soliton molecules, Grelu, Soto-Crespo et al. have performed remarkable experiments and simulations in both anomalous and normal path-averaged cavity dispersion fibre lasers where kinds of bound solitons were observed [18,22,44]. As an example, Figure 13a,b illustrates the temporal and spectral details of a bound state in a laser cavity with normal dispersion-managed configuration. The autocorrelation function in Figure 13a shows a rather triangular shape and the

optical spectrum in Figure 13b presents fully modulated fringe pattern. These two records imply a precise phase locking of closely bound chirped pulses. Numerical efforts verify the conclusion that bound states can be supported regardless of dispersion signs of the cavity.

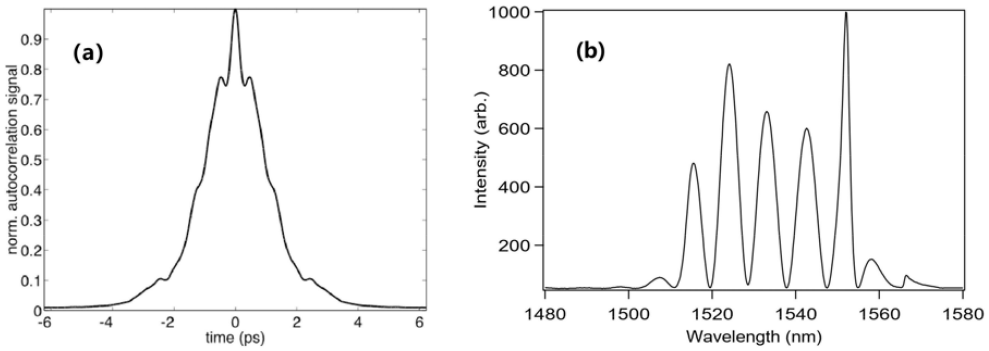

Figure 13. (**a**) Autocorrelation function and (**b**) optical spectrum recorded at one output of the fibre laser in [22]. (Reproduced with permission from [22]. © The Optical Society of America (Washington, DC, USA), 2003).

For a complete overview, Table 1 lists the most relevant experimental observation of two-soliton molecules exhibiting abundant discrete values of phase difference and interpulse separation in diverse configurations of fibre lasers (different wavelengths, difference dispersion conditions, different mode-locking techniques, etc.). At higher pumping power level, soliton molecules consisting of three and more than three solitons as well as bound states of bound solitons have been reported in sorts of fibre lasers [21,27,45–48]. Figure 14 shows two typical examples of such multisoliton complexes observed by Zhao et al. [47]. Indeed, the different peaks of the autocorrelation trace in Figure 14a are equally spaced and exhibit nearly the same width with intensity ratio of 1:2:3:4:5:4:3:2:1, implying that five identical solitons with the same amplitude and width constitute the bound state. In Figure 14b, a two-soliton molecule with pulse separation of about 3 ps behaves as a unit (it is termed twin-pulse in some literatures) and the complete bound state forms by doubling such a unit. The twin-pulses are roughly 8 ps apart from each other in this situation.

Table 1. Experimental observation of two-soliton molecules in mode-locked fibre lasers.

Wavelength	Dispersion	Saturable Absorber	Pulse Width	Pulse Separation	Phase Difference	Reference
1 μm	0.047 ps^2	NPE	4.3 ps	20.33 ps	-	[46]
1 μm	0.0054 ps^2	NPE	0.39 ps	21 ps	-	[48]
1 μm	0.18 ps^2	SESAM	13.4 ps	14.8 ps	$\pi/2$	[49]
1.5 μm	−0.381ps^2	MoS_2	1.2 ps	3.4 ps	π	[33]
1.5 μm	−0.28 ps^2	CNT	0.9 ps	3–20 ps	$\pi, 0, \pm\pi/2$	[28]
1.5 μm	−0.28 ps^2	Graphene	0.62 ps	55 ps	-	[31]
1.5 μm	anomalous	CNT	370 fs	1.5 ps	π	[29]
1.5 μm	−0.1 ps^2	NPE	1.5 ps	18.5 ps	-	[21]
1.55 μm	0.038 ps^2	SESAM	20.3 ps	91 ps	-	[50]
1.55 μm	0.0017 ps^2	CNT	0.18 ps	1.53 ps	$\pm\pi/2$	[51]
1.55 μm	−0.12 ps^2	NALM	1.3 ps	2.2 ps	π	[8]
1.55 μm	anomalous	Soliton shaping	2 ps	5.2 ps	π	[52]
1.5 μm	−0.047 ps^2	NPE	0.58 ps	1.5 ps	π	[53]
1.5 μm	−0.03 ps^2	Graphene	0.307 ps	35 ps	-	[54]
1.5 μm	−0.02 ps^2	CNT	0.71 ps	2.5 ps/3.5 ps	$\pm\pi/2$	[55]
1.5 μm	−0.277 ps^2	Black phosphorus	0.787 ps	7.5 ps	-	[34]
1.5 μm	anomalous	Graphene	0.39 ps	8.1 ps	-	[56]
2 μm	−0.329 ps^2	NPE	0.78 ps	2.5 ps	π	[23]
2 μm	−0.098 ps^2	NPE	0.93 ps	7–15 ps	$\pi, 0$	[24]

NPE: nonlinear polarization evolution; SESAM: semiconductor saturable absorber mirror; MoS_2: molybdenum disulphide; CNT: carbon nanotubes; NALM: nonlinear amplifying loop mirror.

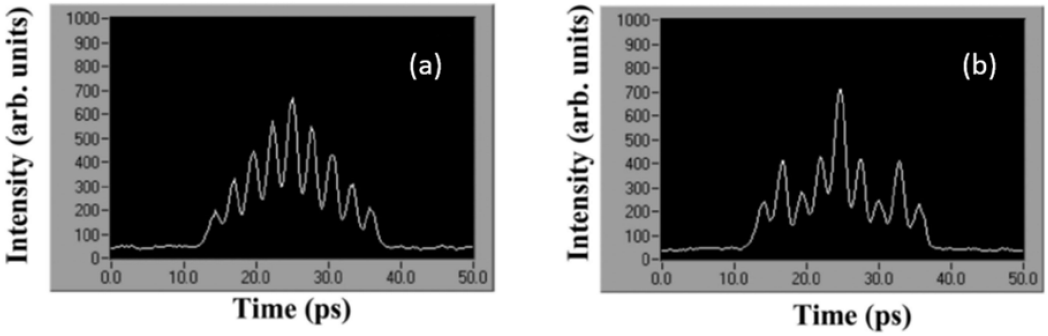

Figure 14. Autocorrelation traces of (**a**) a five-soliton bound state and (**b**) a twin-pulse bound state. (Reproduced with permission from [47]. © The Optical Society of America (Washington , DC, USA), 2007).

Based on a plethora of experimental evidences, it is clear that the state of soliton molecules is one of the intrinsic forms in mode-locked fibre lasers which is independent on cavity details such as dispersion regime, spectral window, saturable absorber and so on. However, the limited variation of experimental parameters implies discreteness and quantization of allowed soliton molecules, meaning that the properties of the attractors in such dissipative systems are sensitive to the detailed features of the systems.

4. Numerical Simulation of Soliton Molecules

The solutions of soliton molecules were first discovered mainly by theoretical analysis of nonlinear Schrödinger equation and complex Ginzburg-Landau equation, which are distributed propagation models and allow a good approximation of the dominating effects in passively mode-locked fibre lasers. Different approaches such as perturbation theory [11], inverse scattering method [57], etc. enable simplified theoretical framework to address the interaction mechanisms and the general behaviours of bound solitons, which were rather controversial in terms of the stability properties [14,15]. Nevertheless, it is noteworthy that those theoretical researches opened exciting avenues for understanding of multipulse interactions in fibre lasers and proved possible capacity scaling in optical communication, inspiring a number of successive experimental findings. For details, see the pioneer work by Malomed, Afanasjev, Akhmediev etc. [11–15,58,59] and references therein.

Later, more and more numerical analysis was made based on lumped model which enables better comparison with experiments since real parametric values such as dispersion and nonlinear Kerr coefficient are involved. Up till now, a plethora of fibre laser cavities with distinct dispersion regimes [19,44], mode-locking techniques [4,60], etc. have been numerically investigated, giving rise to different features of bound states of multiple pulses, for instance, different envelopes and modulation fringes of the optical spectra. The general dynamics of soliton molecules and crucial influences of some cavity parameters have been unravelled in detail, providing fundamental insights into the underlying physics of multisoliton interactions. Some instructive work can be found in refs. [4,5,19,44,60,61].

In this review we would like to demonstrate the basic method of carrying out the numerical simulation of two-soliton molecules. To provide a direct comparison with experiments, impact from several experimentally controllable variables including initial condition, gain and higher-order dispersion are shown respectively. Here we use a modified nonlinear Schrödinger equation based on lumped description of functions of different components. We neglect birefringence and assume a fast saturable absorber in order to simplify numerical calculation without losing the most important impact from cavity parameters. The pulse propagation in gain fibre can be described by a scalar formula

$$i\frac{\partial A}{\partial z} = \frac{\beta_2}{2}\frac{\partial^2 A}{\partial T^2} + i\frac{\beta_3}{6}\frac{\partial^3 A}{\partial T^3} - \gamma|A|^2 A + i\frac{1}{2}\cdot\frac{g_0}{1+E_{pulse}/E_{sat}}(1+T_2{}^2\frac{\partial^2}{\partial T^2})A \quad (6)$$

where A denotes the pulse envelope and T is the time in a frame of reference moving with the group velocity v_g. β_2 and β_3 are the second- and third-order dispersion, γ is the nonlinear Kerr coefficient and g_0 is the small-signal gain. E_{pulse} is the pulse energy while E_{sat} is the saturation energy. Gain dispersion is taken into account in the manner $T_2 = 2\pi/(ck^2\Delta\lambda_g)$ with $\Delta\lambda_g$ being gain bandwidth, in which c is the speed of light in vacuum and k is the wave vector. g_0 is set to zero when the pulses propagate in passive fibres.

The simulated laser cavity is primarily comprised of three segments of optical fibres schematically shown in Figure 15. The erbium-doped fibre provides small-signal gain $g_0 = 3.5\ \mathrm{m}^{-1}$, with saturation energy E_{sat} = 0.5 nJ and gain bandwidth of 80 nm. Other parameters of those three segments of fibres are listed in Table 2. The nonlinear absorption of saturable absorber is expressed by $q = l_0[q_0/(1 + I_p/I_{sat}) + (1 - q_0)]$, where saturation intensity I_{sat} = 20 W, modulation depth q_0 = 0.2 and loss at low incidence power l_0 = 0.5. The output coupling ratio is 30%. Split-step Fourier method is used in the process of numerical calculation. The pulses at the output port are detected and analysed.

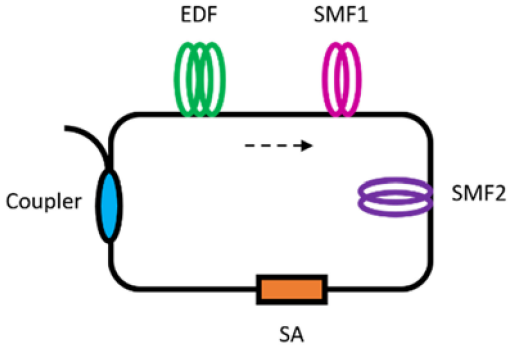

Figure 15. The fibre laser cavity used in simulation. SMF: single-mode fibre. Other abbreviations are the same as those in the main text.

Table 2. Parameters of optical fibres in a fibre laser cavity for numerical simulation.

Fibre Segment	Second-Order Dispersion β_2 (ps^2/km)	Third-Order Dispersion β_3 (ps^3/km)	Nonlinear Kerr Coefficient fl (W^{-1}·km^{-1})	Length L (m)
SMF 1	−7.5	0	2.3	0.2
SMF 2	−22	0	1.2	0.2
EDF	−18	0	3.2	0.4

SMF: single-mode fibre; EDF: erbium-doped fibre.

4.1. Out-of-Phase Two-Soliton Bound States

The initial condition is set as two Gaussian pulses with 1/e pulse width of 200 fs, pulse energy of 1 pJ, pulse separation of 0.1 ps and phase difference of $\pi/2$. As we can see from Figure 16a, the initial noise gets amplified and shaped after numbers of round trips in the cavity and finally converges to a bound state consisting of two identical pulses with fixed separation. Figure 16b depicts the optical spectrum of such soliton molecules in both linear (blue) and logarithmic (orange) scales, giving modulation depth of 100% and modulation period of 11.6 nm. It corresponds to temporal separation of 0.69 ps between the bound solitons, which is also confirmed by the pulse trace in time domain in Figure 16c. In detail, the two pulses are of mirror symmetric profile with respect to each other and they are partly overlapped on their edges. Both optical spectrum and temporal phase information indicate a phase difference of exactly π. In addition, the pulse duration is 0.16 ps, satisfying transform-limited relationship of sech-shaped pulse when relating to the spectral width (time-bandwidth product of 0.315). In this case, the pulse separation is 4.4 times the pulse duration, indicating a strong direct interaction via pulse trail.

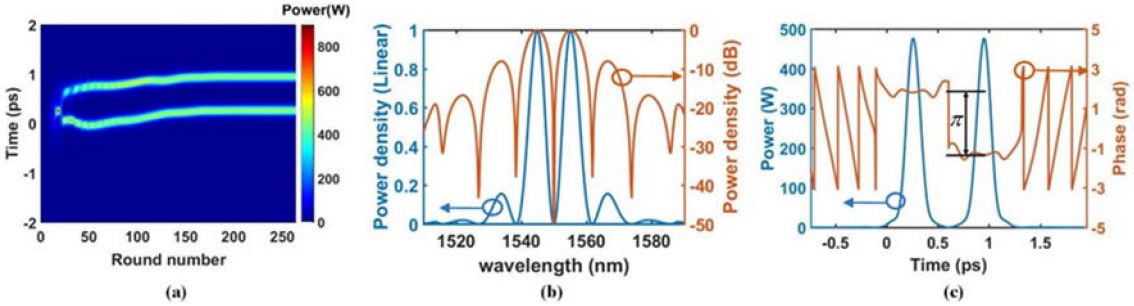

Figure 16. Formation of an out-of-phase bound state and its spectral and temporal properties. (**a**) Evolution process of pulses driven by initial noise; (**b**) Optical spectrum and (**c**) temporal profile of the soliton molecules.

When we set another initial condition, namely, change the phase difference of the two noise pulses to π, the pulse evolution can proceed differently, see Figure 17. The stable state is another soliton molecule state with pulse separation of 3.51 ps and pulse width of 0.15 ps. Therefore, the RSW value is 23.4, making the binding situation looser. It indicates that the initial parameters, i.e., the historical operation status, play an important role in the ultimate steady state of the system. In a dissipative system which contains different attractors, initial situations act in a way somewhat similar to a precursor in chemistry, namely, to guide the system to reach one of the attractors.

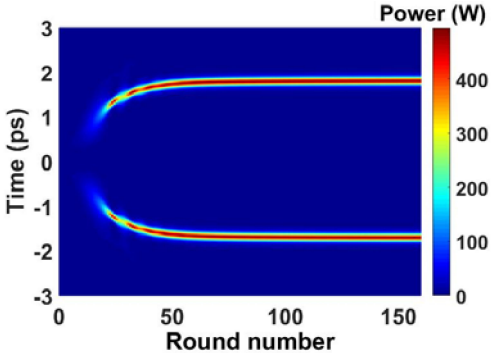

Figure 17. Formation of another out-of-phase bound state initiated by different noise compared to Figure 16.

4.2. In-Phase Two-Soliton Bound States

In-phase soliton molecules can be produced when the initial noise pulses are set in phase, with evolution process shown in Figure 18a. This state exhibits a symmetrical optical spectrum with respect to the central peak (Figure 18b), implying generation of two identical in-phase solitons. The temporal trace in Figure 18c further verifies the in-phase feature. Interestingly, the peaks of Kelly sidebands (marked by green arrows in Figure 18b) coincide perfectly with the peaks of the modulated fringes, suggesting a vital role of dispersive waves in the formation of bound solitons. The interaction length of dispersive waves can be longer than direct interaction by profile overlap in comparison to Figure 16, so that the RSW can be larger too. From the simulation results, we know that the pulse separation is 27.2 times pulse duration, indeed concluding one order of magnitude larger RSW than the case in Figure 16. In addition, the variation of initial phase difference mainly leads to the change of pulse separation, with pulse width nearly constant (0.15 ps here). Similarly, if we set the initial pulse separation to be 1 ps, another in-phase bound state can be achieved, in which the RSW is decreased to 22.7 and the pulse duration is again 0.15 ps (not shown here). These numerical results indicate that the initial conditions affect pulse-pulse interaction more intensively than individual pulses in such a dissipative system.

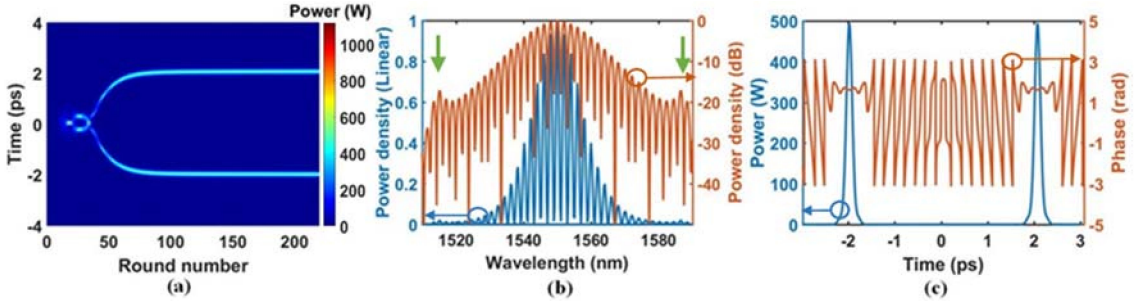

Figure 18. Formation of an in-phase bound state and its spectral and temporal properties. (**a**) Evolution process of pulses driven by initial noise; (**b**) Optical spectrum and (**c**) temporal profile of the soliton molecules.

4.3. Influence of Gain

Here a small-signal gain of 3.3 m^{-1} is used instead of 3.5 m^{-1} on the basis of a steady state in Figure 16. By doing so we want to simulate change of the bound state when decreasing pump power, which we can easily compare with experiment. Change of gain results in simultaneous change of nonlinear effects and therefore transition of the bound state to a new one takes place, as seen in Figure 19. The important hint is that lower gain shapes the pulses with larger temporal distance, meaning that a repulsive force is increased, or an attractive force is decreased. Ref. [4] infers that two pulses get repulsive between each other when we consider cross-phase modulation (XPM) effects in normal dispersion regime by assuming non-coherent interaction, verified by later experimental reports [21]. Similar mechanism holds true here and deduces that XPM effects make two pulses attractive to each other in anomalous dispersion regime, which is indeed what we obtain in our case. When decreasing intracavity gain, the XPM effects are weakened, so that the two solitons get less attractive, achieving a new equilibrium state with larger pulse separation in the end.

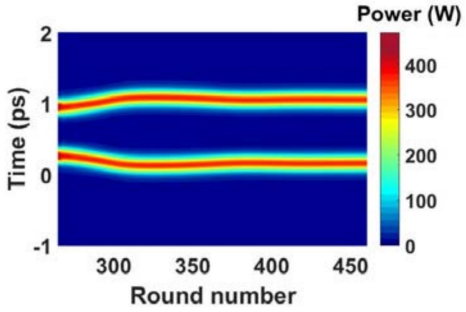

Figure 19. Evolution of a bound state when gain is decreased.

4.4. Influence of Third-Order Dispersion

It is well known that when two closely spaced solitons propagate in an optical fibre, they can attract or repel each other depending on their relative phase [62]. But still, people may ask why such a dissipative system allows solutions with only discrete (more precisely, integer times $\pi/2$) phase differences. What is the magic behind it and what is the possible reason? Actually, when we take higher-order dispersion into account, for instance, here we add third-order dispersion term to this system, we find that the bound solitons do not possess exactly integer times $\pi/2$ phase differences any longer (see Figure 20). The numerical results indicate that the two nearly in-phase bound solitons exhibit a phase difference of 0.126 rad.

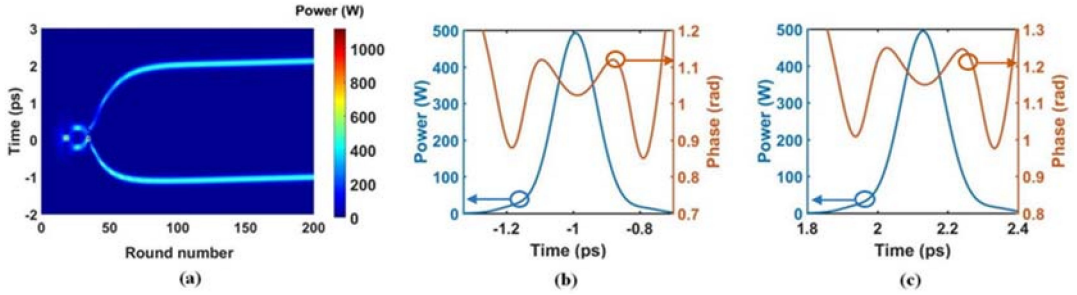

Figure 20. (**a**) Pulse evolution when third-order dispersion is considered. (**b**) and (**c**) show temporal amplitude and phase profile of the two bound solitons, respectively. β_3 = 0.05 ps^3/km, 0.127 ps^3/km and 0.05 ps^3/km for SMF1, SMF2 and EDF, respectively.

Most experiments have claimed approximately perfect integer times $\pi/2$ phase differences in their cavities. One reason is that the phase relationship is usually reflected only by spectral shape, rather than direct measurement of phase by some means like interference, which lacks sufficient accuracy. The other reason is that in most cavities the second-order dispersion dominates, which makes higher-order dispersion neglectable. If a near-zero GVD dispersion laser cavity is investigated, then higher-order dispersion terms might need to be revisited and studied in detail.

It is also worth noting that a fibre laser does not have to ensure complete solutions with all π, 0 and $\pm\pi/2$ phase differences. More often, only π and 0 [63], or only $\pm\pi/2$ [17,44], or only anti-phase [64] solutions have been found in theoretical researches, probably due to limitation of available simulation variables in a single laser cavity. Based on more simulation results from refs. [22,44], we believe that a sole dispersion sign of the cavity is not able to determine or predict the possible phase difference of the solutions. It is rather tricky to select proper parameters for a stable bound state since such an exact balance is reached only when all effects related to gain, loss, nonlinearity and dispersion compromise to a same attractor, which enables soliton molecules an intriguing form in dissipative systems.

5. Discussion on Generation and Stability of Various Soliton Molecules

5.1. Key Parameters for Generation of Soliton Molecules

Gain is the most apparent parameter to tailor in order to operate a fibre laser in the regime of more than one pulse within a round trip. The nonlinear interaction is then the most important and most tricky knob to achieve balanced force between soliton atoms. The complex nonlinear interaction is accomplished by abundant terms, namely, nonlinear terms including nonlinearity of passive fibres, nonlinear gain and nonlinear loss, dispersion terms including second-order and higher-order terms, birefringence terms including linear and nonlinear ones, noise term for instance the initial experimental condition and so on. In experiment, a real saturable absorber, rather than effective one like NPE technique or figure-eight-cavity method, enables an independent control of the interactions between pulses by adjustment of PC orientation with properties of mode-locking pulses (temporal and spectral widths, etc.) almost unchanged. The adjustment of PC orientation could incur change of sidebands [65], therefore cause change of interaction forces between pulses [66–68]. While in other cavities using NPE or NALM techniques, adjustment of wave plates leads to changes of both mode-locker properties and interactions between pulses. The second key reason is the initial conditions. Even though a theoretical solution of in-phase bound states exists in a fibre laser system, an improper initial condition will make the solution unavailable [15]. Before a bound state is generated, control of the initial pulse separation of two-pulse bunch by adjustment of PC orientation is of significant preference. The initial pulse separation could be changed from several nanoseconds to sub-nanosecond (when initial pulse separation was very small, the two-pulse bunch was resolved as a single pulse from the oscilloscope, where real pulse separation is proportional to width of the single pulse displayed by the oscilloscope). Change of the initial pulse separation via PC adjustment may be related to

electrostrictive effect [69] or gain depletion and recovery [70,71], as well as interaction force incurred by dispersive waves [66]. Experimental experiences provide an essential evidence that a bound state was frequently obtained when the initial pulse separation was adjusted to be sub-nanosecond or less, although it is impossible to foresee which kind of bound states will be obtained. By doing so, rather than simply increasing pump power from a single soliton or from cw radiation, a variety of bound states can be experimentally discovered.

5.2. Stability of Soliton Molecules

The short-time stability of bound states can be characterized by measuring RF spectra. It is found that RF spectra of these bound solitons have almost the same signal-to-noise ratio (SNR, larger than 60 dB when 1 kHz span and 1 Hz resolution were set) at the fundamental mode-locking frequency as a single soliton. However, different bound states have different stabilities as far as long-term immunity to environmental perturbation is concerned. Some bound states could only preserve themselves for several minutes before they transformed to unbound states or other bound states. For comparison, some other bound states were able to maintain for at least half an hour or more under perturbations of the lab environment (change of temperature, fluctuation of pump power, etc.).

Generally speaking, soliton molecules with smaller pulse separation have better long-term stabilities (Figure 21 as an example). It is easily understood, as smaller pulse separation guarantees stronger direct mutual interaction between solitons. This can be supported in theory that lower-energy-level (smaller separation) bound states have larger binding energy [7]. However, regarding bound states with similar separation but distinct phase differences, it is rather complicated to foresee which kind (π, 0, $\pi/2$, or $-\pi/2$) is the most stable one. In some situations, the transformation of phase difference from $-\pi/2$ to 0 was observed (also see Figure 21), while in other situations seemingly endless mutual transformation between $-\pi/2$ and $-\pi$ was observed.

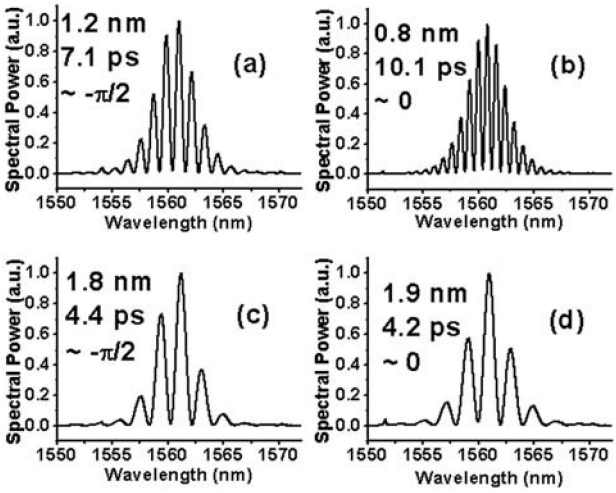

Figure 21. Sequential spectral evolution from (**a**) to (**d**) of a two-soliton bound state under the lab environment without intentional change of experimental conditions. Evolution from (**a**) to (**c**) took several minutes; and (**d**) was stable for at least half an hour. Modulation period, pulse separation and phase difference are marked in the figures. (Reproduced with permission from [28]. © The Optical Society of America (Washington, DC, USA), 2013).

The spectral transition from one soliton-molecule state to the other is of great interest and very instructive. Experimentally, transformation from $-\pi/2$ to 0 was accompanied by overall blue-shift of the envelope of the modulated optical spectrum, while transformation from $-\pi/2$ to $-\pi$ (from $-\pi$ to $-\pi/2$) was accompanied by overall red-shift (blue-shift) of the envelope of the spectrum. These intriguing phenomena imply that transformation of bound states is closely related to slight

change of optical spectra, which stems from change of gain spectrum of the active fibre under fluctuations of ambient temperature [72,73]. Change of phase differences shows good flexibility of bound states to adapt to the environment. Note that phase differences of bound states were not rigorously equal to π, 0 and $\pm\pi/2$ in most cases. As we have shown in the simulation, high-order effects might play a vital role in the complex nonlinear dynamics.

5.3. Interaction Mechanisms

As a particular existing form in ultrafast fibre lasers, soliton molecules result from nonlinear interactions between individual solitons via different parameters of the systems. Similar to the ideas in open systems [3,74] experiencing bidirectional energy exchange with the environment, the dissipative solitons in the dissipative systems of fibre lasers are governed by several effects, namely, dispersion, nonlinearity, gain and loss. In most cases, these effects influence the properties of both single solitons and soliton-soliton interaction in a comprehensive and interdependent fashion, meaning that one cannot simply extract sole impacts from individual terms. One vital example is the relationship between gain and nonlinearity: on the one hand, nonlinearity contains not only the nonlinear Kerr effect from passive fibres but also gain saturation effect from active fibre; on the other hand, since nonlinear Kerr effect is automatically more pronounced with higher gain, variation of gain in experiment leads to variation of nonlinearity. Additionally, it has been reported that the dispersion sign of the gain medium contributes to the stability of soliton molecules [75], indicating that gain and dispersive effects might also be coupled. Similarly, XPM effects can lead to both repulsion and attraction depending on the sign of second-order dispersion. Higher-order dispersion and nonlinearity render pulse-pulse interactions even more complicated.

Although the above-mentioned terms are discussed the most frequently and indeed dominate among abundant fibre laser cavities, anisotropy of the fibre cavity is an additional important parameter to influence bound states. In theory, bound states do exist in scalar framework of dissipative systems. In experiment, however, adjustment of the polarization controllers is usually needed to achieve stable bound solitons, which indicates that the role of birefringence cannot be neglected. Very interestingly, when linear and circular birefringence as well as polarization hole burning effects are taken into account, vector soliton molecules with intriguing polarization dynamics can be observed [29]. Group-velocity-locked vector soliton molecules in a birefringence-enhanced fibre laser have also been experimentally evidenced very recently [76]. Moreover, we want to emphasize the key role of historical status in characteristic properties of bound solitons, a common rule in dissipative systems containing discrete attractors. The initial noise or the initial multipulse state triggers how it will evolve and what is the destination state. In another way, time-dependent response functions by for instance slow saturable absorber and gain recovery connect the original state and the ultimate state as well.

To give a general idea, the sophisticated interactions mediated by different factors are sketched in Figure 22. All these effects (marked by coloured arrows) play key roles in the dissipative optical process, which contribute to an exact balance of all interaction forces and give rise to an equilibrium status of multiple solitons. The properties of individual solitons as well as the characteristic parameters between solitons are determined by the integrated interplay of all effects. In Figure 22, we use a simple mechanical analogy to mimic this optical system, in which two identical balls are equivalent to the identical solitons and the complicated interactions via different factors behave like a spring to enable the two solitons to feel each other.

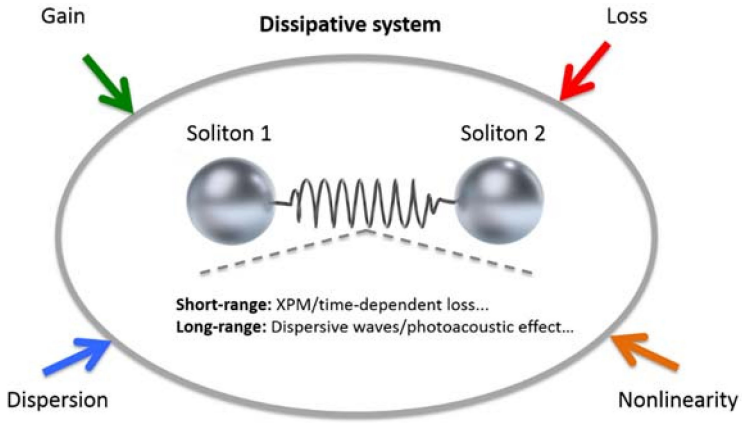

Figure 22. Schematic of soliton molecules generated and stabilized via interactions mediated by different parameters. All factors marked by coloured arrows play important roles in the interactions, hampering a simple interpretation and modelling of the underlying physical mechanisms. However, a systematic analysis of the interaction forces at different length scales provides significant insights.

Despite of the complexity of the interplay, it is rather instructive to analyse the interaction process at different length scales. Depending on the spatial relationship of multiple pulses, short- or long-range physical mechanisms can dominate in the interactions respectively (several examples are listed in Figure 22). When the neighbouring pulses are close to each other, direct and strong soliton-soliton interaction takes place. In this region, Komarov et al. have found the important role of the oscillatory tails of single solitons [77,78], via which the discrete bound states are determined by quantized local minima of nonlinear losses [7]. Based on their theoretical frame, the effective interaction potential enables prediction of the existence of in-, opposite- and $\pi/2$-phase bound solitons. Among the specific interaction terms, nonlinear Kerr and Raman effects [79] dominate, concerning their response time on the order of tens of femtoseconds (for silica fibre, the response time of the Kerr nonlinearity is <10 fs and Raman 60–70 fs [62]). Those nonlinear effects lead to change of mutual frequency content of the partially overlapped pulses and dispersive effects lead to change of group velocity. Depending on the sign of the dispersion, the adjacent solitons can then repel or attract each other. Because dispersion distribution is usually inhomogeneous inside a fibre laser, particularly in the case of dispersion-managed cavities, so that solitons exhibit strong stretching and compression when travelling along the cavity. Therefore the nonlinear effects via pulse overlapping can play a role typically in the range of several to several tens of times pulse duration [19], or say, several picoseconds. Another short-range interaction is mediated by saturable absorption recovery time, i.e., the time-dependent loss on a timescale of femtoseconds to picoseconds, typical of most effective and natural saturable absorbers.

Simultaneously, indirect interaction is very common via long-range media such as dispersive waves, continuous-wave emission [31] and acoustic waves [69,80]. They influence interaction forces by again changing the refractive indices of the optical fibres, so that widely spaced pulses are able to feel each other and possess distinct group velocities. Such long-range media are typically responsible for the weak interaction on a scale of picoseconds to microseconds.

The key role of dispersive waves in formation of bound states has attracted great attention. In anomalous dispersion regime, periodic soliton reshaping results in the radiation of dispersive waves. The phase-matched interaction at specific frequencies between soliton and radiation components produces resonant sidebands of significant magnitude, known as Kelly sidebands of fibre lasers [81,82]. As an example to unravel the vital impact of dispersive waves, Figure 23 shows the optical spectra of several bound states in a 2 μm fibre laser similar to Figure 9. Remarkably, the Kelly sidebands perfectly coincide with the interference fringes of the spectrum, yielding integer number of interference fringes between the two lowest-order Kelly sidebands (see Figure 23a,c). Induced by a slight perturbation

on the pumping power, the little deviation from the obtained equilibrium point of the soliton pair, with the pulse separation of ~7.2 ps (Figure 23b), eventually evolves into another equilibrium point (Figure 23d). These experimental results provide clear evidence to the importance of dispersive waves on formation of bound states and confirm that the quantized separation is a universal property of the phase-locked solitons [18,19]. The internal repulsion or attraction between two pulses of the soliton pair, which is induced by the process of soliton-continuum interaction, is a periodical function of the initial pulse separation with a set of equilibrium point, where the repulsion and attraction balance each other.

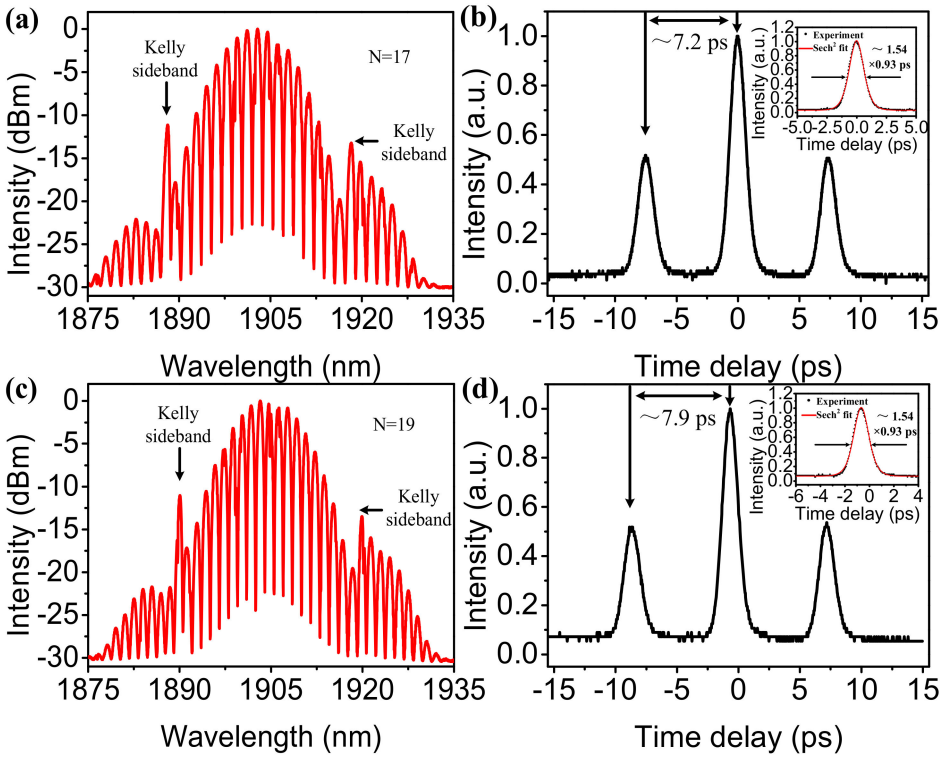

Figure 23. Experimental evidence of the important impact from dispersive waves: optical spectrum with (**a**) 17 interference fringes and (**c**) 19 interference fringes between the two lowest-order Kelly sidebands; optical autocorrelation trace (inset: magnified view of the central peak fitted by sech^2 profile) with (**b**) 17 interference fringes and (**d**) 19 interference fringes between the two lowest-order Kelly sidebands. (Reproduced with permission from [24]. © The Optical Society of America (Washington, DC, USA), 2017).

In addition, it has been discovered that transient depletion and recovery dynamics of the gain medium provides an effective repulsive force between adjacent solitons by imparting a group velocity drift proportional to the inter-pulse spacing [70]. Overall, this long-range effect is usually very weak and incoherent and most likely drives multiple pulses to the states of irregularly ordered pulse bunching and harmonic mode-locking. The interaction length can be of the order of microseconds in time domain.

6. Other Multisoliton States and Dissipative Soliton Dynamics

Precisely, a so-called soliton molecule in this Review as a type of bound state is characterized by constant pulse separation and invariant phase difference over a huge number of round trips, which results from an exact balance between forces. More generally, bound states can manifest themselves with many types, e.g., variant parameters of phase difference and temporal displacement, which have been widely found and discussed. To name a few, vibrating solitons [83,84] exhibit change

of both pulse separation and phase difference within a small range, oscillating bound states [85] possess a periodic oscillation of temporal separation or phase difference or pulse amplitude and bound states with independently evolving phase [5,86] or flipping phase [86] are additionally available. Furthermore, presence of soliton molecules together with a single soliton [20], harmonic mode-locking of two-soliton bound states [33], bound states of two pulse groups (each group is composed of two bound solitons, or say twin-pulse as mentioned before) [87], bunching of soliton molecules, etc. has been extensively verified in experiment. Those multisoliton complexes again reflect the potential sophisticated interactions and dynamics in fibre lasers owing to the dissipative nature of such systems.

In addition, there are many other complex dissipative soliton dynamics in mode-locked fibre lasers. Here we briefly introduce some of them, including vibrating soliton pairs (VSP), soliton rains, rogue waves and coexisting dissipative solitons which we mainly focused on. On the one hand those investigations on multisoliton states provide more insight into the multiple pulse dynamics and output diversity in fibre lasers, showing the intriguing and different possibilities for practical applications. On the other hand, they demonstrate also the challenge and difficulties that we have to overcome in order to fully manipulate and stabilize the interactions between solitons.

In a dissipative system, the presence of soliton molecules as stationary soliton pairs is linked to the existence of fixed point attractors [3]. In contrast, the complexity of the dissipation nature can also lead to limit cycle as supercritical Hopf-type bifurcation [23,83], which is linked to vibrating soliton pairs.

By altering the cavity parameters shown in Figure 9, the nature of the dynamical attractor is changed from a fixed point to a limit cycle through a Hopf-type bifurcation [23,83], generating vibrating soliton pairs. The optical spectrum features a modulation period of about 3.6 nm (Figure 24a). The central dip in the symmetric structure suggests a dominant π-phase difference. As shown in Figure 24b, the corresponding autocorrelation trace reveals broadened cross-correlation peaks at the 3.56 ps pulse separation. The measured FWHM of these side peaks is 1.46 $\pm$ 0.01 ps, markedly larger than the 1.26-ps FWHM of the central peak. The intensity ratio of the three peaks is no longer 1:2:1 and the amplitude of the side peak is reduced, which is consistent with their broadening. The results reflect the time averaging of a VSP dynamics [83]. The RF spectrum in Figure 24d exhibits tiny symmetrical sidebands located around 630 Hz apart from the main peak, which is a low-frequency pulsation typical of VSPs.

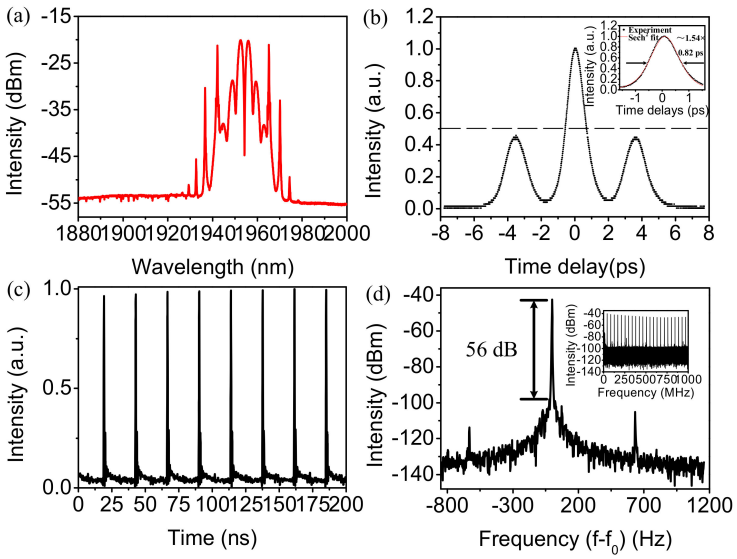

Figure 24. Experimental observation of a vibrating soliton pair at ~1950 nm: (**a**) optical spectrum; (**b**) optical autocorrelation trace (inset: magnified view of the central peak fitted by sech^2 profile); (**c**) pulse train on oscilloscope; (**d**) RF spectrum (inset: RF spectrum over a 1-GHz span). (Reproduced with permission from [23]. © The Optical Society of America (Washington, DC, USA), 2016).

Soliton rains were first observed in an anomalous dispersion Er-doped fibre laser [88–90]. The name originates from the analogy to evaporative cycle of the water [89]. In a soliton rain, multiple closely spaced dissipative solitons form a condensed phase; new weak dissipative solitons (termed as drifting dissipative solitons afterwards) arise from the noisy background spontaneously and drift towards the condensed phase, collide and annihilate. Multiple solitons (several tens) generation and different operation centre frequencies between the condensed phase and the drifting solitons (related to relative drift) are two requirements of soliton rains [89]. These two requirements can be easily satisfied in the anomalous dispersion regime. Hence, it was first observed in anomalous dispersion fibre lasers.

In contrast, it is more difficult to get multiple solitons operation in the normal dispersion regime under a moderate pump power, as pulse propagating in the normal dispersion tolerates larger nonlinear phase shift [91]. By using a dual-filter design, soliton rains were also observed in a normal dispersion fibre laser (Figure 25a) [92]. The dual-filter consists of a narrowband Gaussian filter and a broadband, multiple transmission peak birefringent filter. The narrowband filter enables the mode-locked pulse break into multiple pulses easily [92,93]. The multiple transmission peak filter causes the emission of dissipative solitons in the condensed phase and the drifting dissipative solitons at different centre wavelengths. Thus, they can have relative move due to the difference in group velocity.

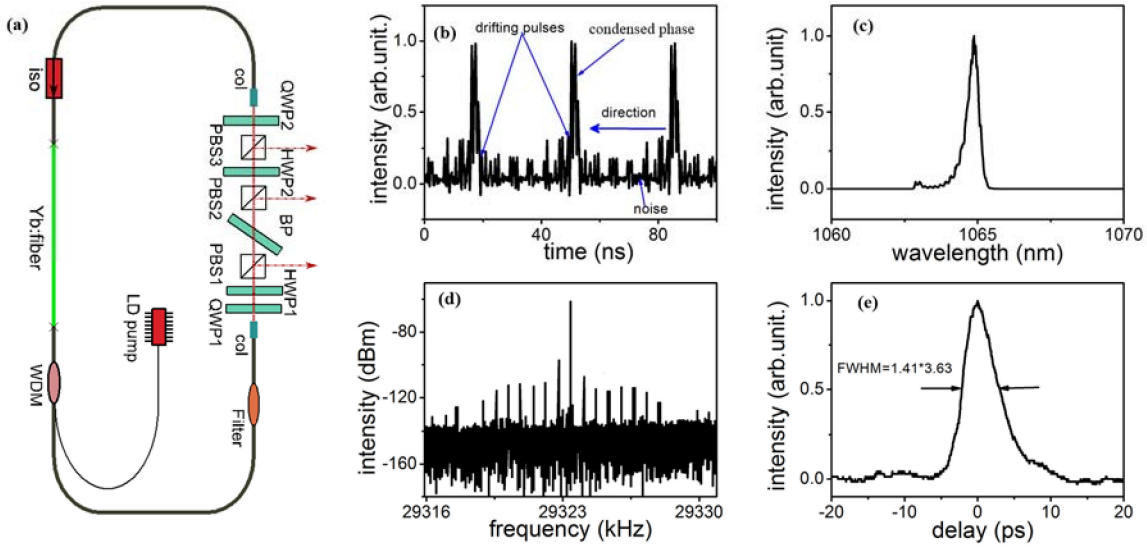

Figure 25. (**a**) Illustration of the mode-locked Yb-fibre laser with dual-filter for observing soliton rains. iso: isolator, WDM: wavelength division multiplexer, PBS: polarization beam splitter, QWP: quarter waveplate, HWP: half waveplate, BP: birefringent plate; (**b**) Temporal trace of soliton rains, showing that the drifting solitons move towards a condensed phase; (**c**) Optical spectrum of the state; (**d**) RF spectrum of the state; (**e**) Autocorrelation trace of the soliton rain state. (Reproduced with permission from [92]. © The Optical Society of America (Washington, DC, USA), 2013).

Figure 25b is the measured temporal trace of the soliton rain state, showing a similar temporal dynamic to those in anomalous dispersion regime. The mode-locked spectrum is relatively narrow (Figure 25c) and the measured RF spectrum reflects the complex temporal dynamics. The measured autocorrelation trace shows the multiple pulses are relatively far spaced, different from a typical soliton-molecule state.

Rogue waves (RWs) are extreme waves that exceed expectation based on long-term observation and Gaussian statistics. In particular, optical RWs go beyond the significant wave height by a factor of 2, which have been widely investigated in different nonlinear optical systems, such as mode-locked Ti:sapphire lasers [94], Raman fibre amplifiers [95,96], parametric processes [97] and fibre lasers [98–106]. Figure 26 shows typical characterizations of dissipative RWs, which were obtained

in a Tm-doped fibre laser mode-locked by monolayer MoS_2 [107]. The net GVD of the cavity is approximately -3.82 ps^2. Under enough pumping and appropriate PC settings, the pulses become aggregated as a bunch of intense pulses with internal structure fluctuating, namely noise-like pulses (NLPs). The features of NLPs can be significantly affected by the polarization state of the PCs. Effective cavity spectral filtering related to the intracavity elements of the PCs and the effective birefringence [108], modifies both the spectral width and the overall shape of the optical spectrum of NLPs. Figure 26a presents typical example of pulse-energy fluctuations over successive round trips. One particularly large and localized energy fluctuation can be observed on the left part of the pulse recordings. When recording approximately 500 thousand of trace samples on the oscilloscope, a significant deviation can be observed from Gaussian statistics in high-amplitude part with long tail in the histogram of Figure 26e. The significant wave height (SWH) is defined as the mean amplitude of the highest third of the waves [99,101]. The highest recorded amplitude is 1596.5 mV, around 2.36 times that of the SWH of 677.4 mV, revealing the generation of DRWs. The proportion of the DRWs is about 0.11%. The autocorrelation trace is also measured, exhibiting coherence spike upon wide pedestal that extends over the entire width of the measurement window. The RF spectrum in Figure 26d also reflects typical feature of the NLPs regime.

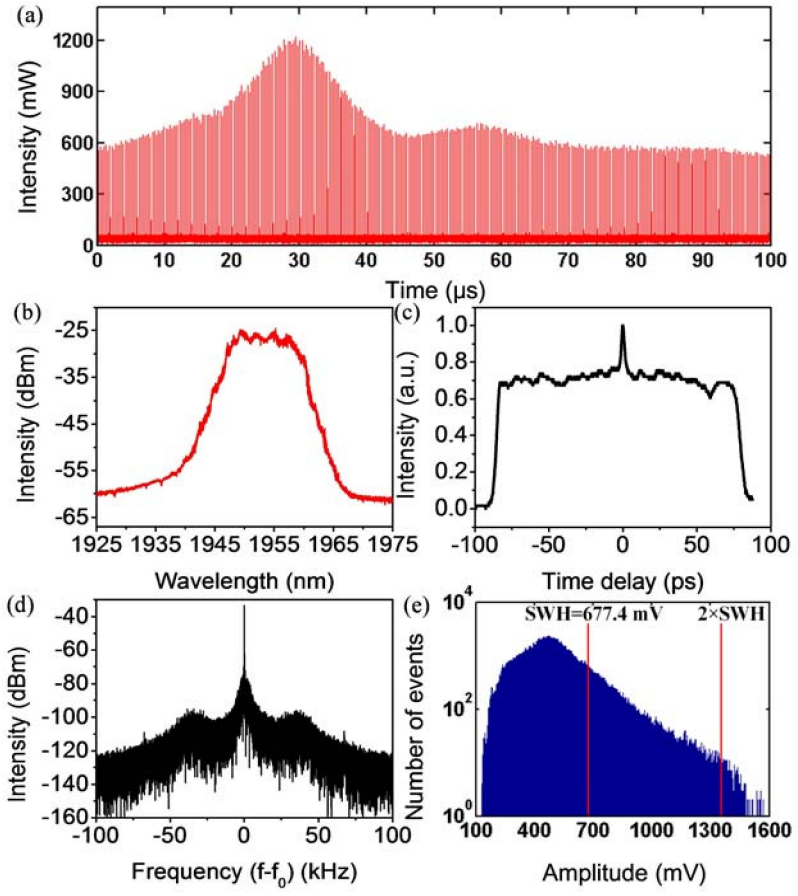

Figure 26. Dissipative rogue waves in a Tm-doped fibre laser: (**a**) temporal sequences of output pulse recordings; (**b**) optical spectrum; (**c**) autocorrelation trace; (**d**) RF spectrum over a 200 kHz span with resolution bandwidth of 10 Hz; (**e**) histogram on log scale showing the distribution of the pulse energy. (© 2018 IEEE, Piscataway, NJ, USA. Reprinted, with permission from [107]).

In the above, we mainly discuss complex dissipative soliton dynamics with multiple dissipative solitons in the cavity. When a single pulse propagates in the laser cavity, it can also exhibit complicated dynamics. For instance, a single pulse can experience soliton explosion in mode-locked laser [109–111].

In a soliton explosion, dissipative soliton intermittently (but non-periodic) undergoes an explosive state (sudden change of some parameters in the frequency and time domain) and returns to the original state. Presently, we introduce a state where single dissipative soliton can operate in the bistable coexisting state for a single set of system parameters [112]. This coexisting dissipative solitons can be understood as state that multiple stable soliton solutions coexist and the mode-locked laser is switching between them [112]. When coexisting dissipative solitons occur, a mode-locked pulse is switching within two states with distinct spectra (spectrum shape, centre frequency and spectral bandwidth) and pulse energy spontaneously (see Figure 27a–c). Numerical simulations based on a master equation, which is a quintic complex Swift-Hohenberg equation [113], reproduce the observed phenomena (Figure 27d,e). The simulations also unveil that the double minima frequency loss (corresponds to a birefringent plate filter in the laser cavity) is critical to the observed switching. The observation of coexisting dissipative solitons gives a good example of how multiple solutions can be stable simultaneously in a dissipative system.

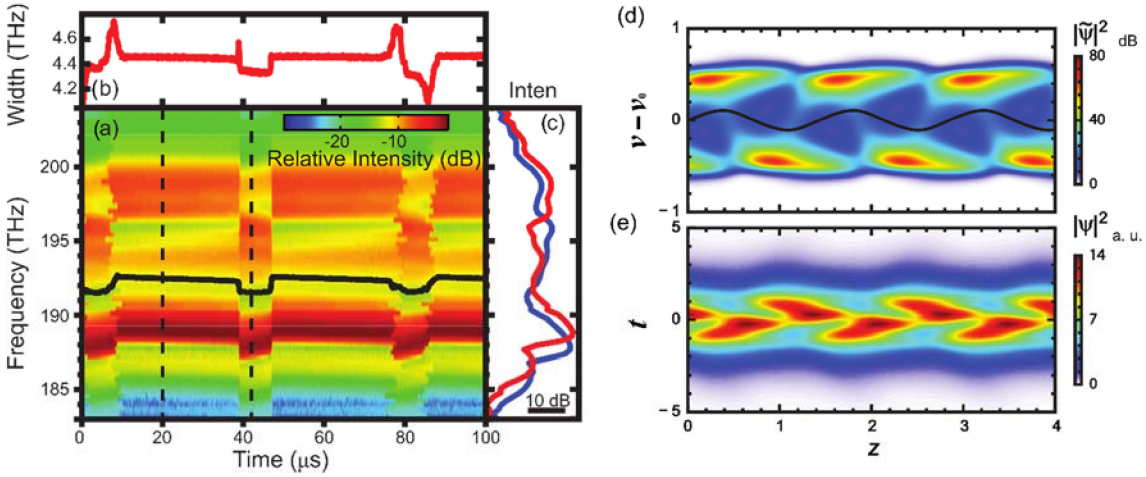

Figure 27. Experimental and numerical observation of the coexisting dissipative solitons. (**a**) Measured fast switch of the spectrum of the coexisting dissipative solitons obtained by selecting spectral slice using a monochromator and recording the power trace; (**b**) Calculated spectral bandwidth of the spectrum; (**c**) Two typical spectra, represented by the dashed line in (**a**) at 20 μs and 42 μs of the recorded spectrum, showing a change over 1 THz in the centre frequency; (**d**) Numerical simulated switching of the spectrum of the mode-locked state; (**e**) The corresponding temporal evolution of the simulation result. Associated with the spectral switching, the pulse is advanced and slowed due to the centre-frequency shift induced group-velocity change via dispersion. (Reproduced with permission from [112]. © The American Physical Society (College Park, MD, USA), 2015).

7. Conclusion and Outlook

In this review, we summarize the latest experimental researches on soliton molecules and other multisoliton states in mode-locked fibre lasers. As a promising equilibrium phase of multiple pulses potentially significant to developing high-capacity telecommunication, soliton molecules are stationary pulse pairs stemming from balanced forces by dissipation nature of fibre lasers, forming bound states with invariant interpulse temporal separation as well as discretely fixed phase relationship. Independent of cavity details for example working wavelength, dispersion scheme and mode-locking technique, soliton molecules exist in general as an intrinsic allowed status in fibre lasers. However, sensitive to cavity parameters such as saturation gain, initial condition, etc., soliton molecules can manifest themselves with distinct pulse separation, which can be one to two orders of magnitude as large as pulse width depending on the interaction length of the dominating effects. The phase relationship between solitons mainly locates among in-phase, out-of-phase and $\pm\pi/2$ phase difference, since second-order dispersion leads dispersive terms. Numerical efforts based on modified nonlinear

Schrödinger equation and lumped description method have been made to unveil key roles of historical status, gain and dispersion in formation of bound solitons and their characteristic parameters. Experimental control for efficient generation of soliton molecules and their stabilities are discussed in detail. The complicated interaction mechanisms are additionally addressed.

In comparison to the stationary boundary states which are one of the simplest existence states, the complex dissipation dynamics in fibre lasers can lead to many other kinds of multisoliton states and dissipative phenomena including vibrating soliton pairs, soliton rains, rogue waves, bistable coexisting states and so on. Such soliton complexes involving diverse nonlinear behaviours are not only of fundamental interest but also of practical importance, for instance, in applications related to chaos, optical storage and optical switching.

The versatility of fibre laser cavities has enriched physical understanding of multipulse interaction mechanisms and realistic findings on generation and control of multiple solitons in such dissipative systems. However, the numerous experimental variables and the limited characterization measures hamper a general description of all discoveries in experiment to date, making a complete dynamics analysis very challenging. Especially when we study such nonlinear optical phenomena at both macroscopic and microscopic levels, namely, at different time scales addressing pulse trains and individual pulses, a precise description of soliton complexes becomes a very tough task. In the future, we anticipate that more experimental reports and more theoretical framework will be carried out. More optical measurement methods will be developed in order to provide worthy means for detailed recording of the properties of multisoliton ensembles such as phase information. Very recent breakthrough experiments on time-stretch dispersive Fourier transform techniques enable a real-time observation of build-up and evolution process of soliton molecules [9,10], which will be applied and tested in more systems and situations. In addition, some trials on long-distance transmission of soliton molecules and coding in multiple solitons for example by means of manipulation on polarization states may promote related developments and pave the way towards real applications. We are convinced that the complex dissipation phenomena will be further explored and might go beyond what we know and what we expect at this moment, from the both sides of fundamental physics and applied optics.

Acknowledgments: This work was financially supported by the National Natural Science Foundation of China (NSFC) (61377039, 61575106 and 51527901). Lili Gui additionally acknowledges financial support from the Carl-Zeiss-Stiftung for her research in Germany. Chengying Bao acknowledges a fellowship from the Resnick Institute, Caltech.

Author Contributions: Lili Gui and Changxi Yang conceived the original idea; Lili Gui, Pan Wang and Chengying Bao summarized and analysed the main experimental results; Lili Gui, Yihang Ding and Kangjun Zhao analysed the state of the art and contributed to numerical simulation; Lili Gui, Changxi Yang, Pan Wang and Chengying Bao discussed the nonlinear interaction mechanisms; all authors discussed and wrote this manuscript.

Conflicts of Interest: The authors declare no conflict of interest. The founding sponsors had no role in the design of the study; in the collection, analyses, or interpretation of data; in the writing of the manuscript and in the decision to publish the results.

References

1. Xu, C.; Wise, F. Recent advances in fibre lasers for nonlinear microscopy. *Nat. Photonics* **2013**, *7*, 875–882. [CrossRef] [PubMed]
2. Fermann, M.E.; Hartl, I. Ultrafast fibre lasers. *Nat. Photonics* **2013**, *7*, 868–874. [CrossRef]
3. Grelu, P.; Akhmediev, N. Dissipative solitons for mode-locked lasers. *Nat. Photonics* **2012**, *6*, 84–92. [CrossRef]
4. Olivier, M.; PichÚ, M. Origin of the bound states of pulses in the stretched-pulse fibre laser. *Opt. Express* **2009**, *17*, 405–418. [CrossRef] [PubMed]
5. Ortaç, B.; Zaviyalov, A.; Nielsen, C.K.; Egorov, O.; Iliew, R.; Limpert, J.; Lederer, F.; Tünnermann, A. Observation of soliton molecules with independently evolving phase in a mode-locked fibre laser. *Opt. Lett.* **2010**, *35*, 1578–1580. [CrossRef] [PubMed]
6. Stratmann, M.; Pagel, T.; Mitschke, F. Experimental observation of temporal soliton molecules. *Phys. Rev. Lett.* **2005**, *95*, 143902. [CrossRef] [PubMed]

7. Komarov, A.; Komarov, K.; Sanchez, F. Quantization of binding energy of structural solitons in passive mode-locked fibre lasers. *Phys. Rev. A* **2009**, *79*, 033807. [CrossRef]
8. Yun, L.; Liu, X. Generation and propagation of bound-state pulses in a passively mode-locked figure-eight laser. *IEEE Photonics J.* **2012**, *4*, 512–519.
9. Herink, G.; Kurtz, F.; Jalali, B.; Solli, D.R.; Ropers, C. Real-time spectral interferometry probes the internal dynamics of femtosecond soliton molecules. *Science* **2017**, *356*, 50–54. [CrossRef] [PubMed]
10. Krupa, K.; Nithyanandan, K.; Andral, U.; Tchofo-Dinda, P.; Grelu, P. Real-time observation of internal motion within ultrafast dissipative optical soliton molecules. *Phys. Rev. Lett.* **2017**, *118*, 243901. [CrossRef] [PubMed]
11. Malomed, B.A. Bound solitons in the nonlinear Schrödinger-Ginzburg-Landau equation. *Phys. Rev. A* **1991**, *44*, 6954–6957. [CrossRef] [PubMed]
12. Malomed, B.A. Bound solitons in coupled nonlinear Schrödinger equations. *Phys. Rev. A* **1992**, *45*, R8321–R8323. [CrossRef] [PubMed]
13. Afanasjev, V.V.; Akhmediev, N. Soliton interaction in nonequilibrium dynamical systems. *Phys. Rev. E* **1996**, *53*, 6471–6475. [CrossRef]
14. Afanasjev, V.V.; Malomed, B.A.; Chu, P. Stability of bound states of pulses in the Ginzburg-Landau equations. *Phys. Rev. E* **1997**, *56*, 6020. [CrossRef]
15. Akhmediev, N.; Ankiewicz, A.; Soto-Crespo, J. Multisoliton solutions of the complex Ginzburg-Landau equation. *Phys. Rev. Lett.* **1997**, *79*, 4047–4051. [CrossRef]
16. Tang, D.Y.; Man, W.S.; Tam, H.Y.; Drummond, P.D. Observation of bound states of solitons in a passively mode-locked fibre laser. *Phys. Rev. A* **2001**, *64*, 033814. [CrossRef]
17. Tang, D.Y.; Zhao, B.; Shen, D.Y.; Lu, C.; Man, W.; Tam, H. Compound pulse solitons in a fibre ring laser. *Phys. Rev. A* **2003**, *68*, 013816. [CrossRef]
18. Grelu, P.; Belhache, F.; Gutty, F.; Soto-Crespo, J. Phase-locked soliton pairs in a stretched-pulse fibre laser. *Opt. Lett.* **2002**, *27*, 966–968. [CrossRef] [PubMed]
19. Zhao, L.; Tang, D.; Wu, X.; Lei, D.; Wen, S. Bound states of gain-guided solitons in a passively mode-locked fibre laser. *Opt. Lett.* **2007**, *32*, 3191–3193. [CrossRef] [PubMed]
20. Ortac, B.; Hideur, A.; Brunel, M.; Chedot, C.; Limpert, J.; Tunnermann, A.; Ilday, F.O. Generation of parabolic bound pulses from a Yb-fibre laser. *Opt. Express* **2006**, *14*, 6075–6083. [CrossRef] [PubMed]
21. Peng, J.; Zhan, L.; Luo, S.; Shen, Q.S. Generation of soliton molecules in a normal-dispersion fibre laser. *IEEE Photonics Technol. Lett.* **2013**, *25*, 948–951. [CrossRef]
22. Grelu, P.; Béal, J.; Soto-Crespo, J. Soliton pairs in a fibre laser: From anomalous to normal average dispersion regime. *Opt. Express* **2003**, *11*, 2238–2243. [CrossRef] [PubMed]
23. Wang, P.; Bao, C.Y.; Fu, B.; Xiao, X.S.; Grelu, P.; Yang, C.X. Generation of wavelength-tunable soliton molecules in a 2-mu m ultrafast all-fibre laser based on nonlinear polarization evolution. *Opt. Lett.* **2016**, *41*, 2254–2257. [CrossRef] [PubMed]
24. Wang, P.; Xiao, X.; Yang, C. Quantized pulse separations of phase-locked soliton molecules in a dispersion-managed mode-locked Tm fibre laser at 2 μm. *Opt. Lett.* **2017**, *42*, 29–32. [CrossRef] [PubMed]
25. Seong, N.; Kim, D. Experimental observation of stable bound solitons in a figure-eight fibre laser. *Opt. Lett.* **2002**, *27*, 1321–1323. [CrossRef] [PubMed]
26. Nielsen, C.K.; Ortac, B.; Schreiber, T.; Limpert, J.; Hohmuth, R.; Richter, W.; Tunnermann, A. *Fibre Lasers III: Technology, Systems and Applications Vol. 6102 Proceedings of the Society of Photo-Optical Instrumentation Engineers (SPIE)*; Brown, A.J.W., Nilsson, J., Harter, D.J., Tunnermann, A., Eds.; SPIE International Society for Optics and Photonics: Bellingham, WA, USA, 2006; p. 10217.
27. Wu, X.; Tang, D.; Luan, X.; Zhang, Q. Bound states of solitons in a fibre laser mode locked with carbon nanotube saturable absorber. *Opt. Commun.* **2011**, *284*, 3615–3618. [CrossRef]
28. Gui, L.; Xiao, X.; Yang, C. Observation of various bound solitons in a carbon-nanotube-based erbium fibre laser. *J. Opt. Soc. Am. B Opt. Phys.* **2013**, *30*, 158–164. [CrossRef]
29. Tsatourian, V.; Sergeyev, S.V.; Mou, C.B.; Rozhin, A.; Mikhailov, V.; Rabin, B.; Westbrook, P.S.; Turitsyn, S.K. Polarisation dynamics of vector soliton molecules in mode locked fibre laser. *Sci. Rep.* **2013**, *3*, srep03154. [CrossRef] [PubMed]
30. Li, X.; Zhang, S.; Meng, Y.; Hao, Y.; Li, H.; Du, J.; Yang, Z. Observation of soliton bound states in a graphene mode locked erbium-doped fibre laser. *Laser Phys.* **2012**, *22*, 774–777. [CrossRef]

31. Gui, L.; Li, X.; Xiao, X.; Zhu, H.; Yang, C. Widely spaced bound states in a soliton fibre laser with graphene saturable absorber. *IEEE Photonics Technol. Lett.* **2013**, *25*, 1184–1187. [CrossRef]
32. Luo, A.P.; Liu, H.; Zhao, N.; Zheng, X.W.; Liu, M.; Tang, R.; Luo, Z.C.; Xu, W.C. Observation of Three Bound States From a Topological Insulator Mode-Locked Soliton Fibre Laser. *IEEE Photonics J.* **2014**, *6*, 1–8. [CrossRef]
33. Wang, Y.; Mao, D.; Gan, X.; Han, L.; Ma, C.; Xi, T.; Zhang, Y.; Shang, W.; Hua, S.; Zhao, J. Harmonic mode locking of bound-state solitons fibre laser based on MoS_2 saturable absorber. *Opt. Express* **2015**, *23*, 205–210. [CrossRef] [PubMed]
34. Wang, Z.; Xu, Y.; Dhanabalan, S.C.; Sophia, J.; Zhao, C.; Xu, C.; Xiang, Y.; Li, J.; Zhang, H. Black phosphorus quantum dots as an efficient saturable absorber for bound soliton operation in an erbium doped fibre laser. *IEEE Photonics J.* **2016**, *8*, 1503310. [CrossRef]
35. Gui, L.; Yang, X.; Zhao, G.; Yang, X.; Xiao, X.; Zhu, J.; Yang, C. Suppression of continuous lasing in a carbon nanotube polyimide film mode-locked erbium-doped fibre laser. *Appl. Opt.* **2011**, *50*, 110–115. [CrossRef] [PubMed]
36. Wang, Q.; Chen, T.; Li, M.; Zhang, B.; Lu, Y.; Chen, K.P. All-fibre ultrafast thulium-doped fibre ring laser with dissipative soliton and noise-like output in normal dispersion by single-wall carbon nanotubes. *Appl. Phys. Lett.* **2013**, *103*, 011103. [CrossRef]
37. Wang, X.; Zhou, P.; Wang, X.; Xiao, H.; Liu, Z. Pulse bundles and passive harmonic mode-locked pulses in Tm-doped fibre laser based on nonlinear polarization rotation. *Opt. Express* **2014**, *22*, 6147–6153. [CrossRef] [PubMed]
38. Xu, Y.; Song, Y.-L.; Du, G.-G.; Yan, P.-G.; Guo, C.-Y.; Zheng, G.-L.; Ruan, S.-C. Soliton dynamic patterns of a passively mode-locked fibre laser operating in a 2 μm region. *Laser Phys. Lett.* **2015**, *12*, 045108. [CrossRef]
39. Bao, C.; Yang, C. Harmonic mode-locking in a tm-doped fibre laser: Characterization of its timing jitter and ultralong starting dynamics. *Opt. Commun.* **2015**, *356*, 463–467. [CrossRef]
40. Chernysheva, M.; Bednyakova, A.; Al Araimi, M.; Howe, R.C.T.; Hu, G.H.; Hasan, T.; Gambetta, A.; Galzerano, G.; Rummeli, M.; Rozhin, A. Double-Wall Carbon Nanotube Hybrid Mode-Locker in Tm-doped Fibre Laser: A Novel Mechanism for Robust Bound-State Solitons Generation. *Sci. Rep.* **2017**, *7*, srep44314. [CrossRef] [PubMed]
41. Zhao, L.; Tang, D.; Cheng, T.; Lu, C. Gain-guided solitons in dispersion-managed fibre lasers with large net cavity dispersion. *Opt. Lett.* **2006**, *31*, 2957–2959. [CrossRef] [PubMed]
42. Zhao, L.; Tang, D.; Wu, J. Gain-guided soliton in a positive group-dispersion fibre laser. *Opt. Lett.* **2006**, *31*, 1788–1790. [CrossRef] [PubMed]
43. Ilday, F.; Buckley, J.; Clark, W.; Wise, F. Self-similar evolution of parabolic pulses in a laser. *Phys. Rev. Lett.* **2004**, *92*, 213902. [CrossRef] [PubMed]
44. Grelu, P.; Belhache, F.; Gutty, F.; Soto-Crespo, J.M. Relative phase locking of pulses in a passively mode-locked fibre laser. *J. Opt. Soc. Am. B Opt. Phys.* **2003**, *20*, 863–870. [CrossRef]
45. Zhao, B.; Tang, D.; Shum, P.; Guo, X.; Lu, C.; Tam, H. Bound twin-pulse solitons in a fibre ring laser. *Phys. Rev. E* **2004**, *70*, 067602. [CrossRef] [PubMed]
46. Ortaç, B.; Hideur, A.; Chartier, T.; Brunel, M.; Grelu, P.; Leblond, H.; Sanchez, F. Generation of bound states of three ultrashort pulses with a passively mode-locked high-power Yb-doped double-clad fibre laser. *IEEE Photonics Technol. Lett.* **2004**, *16*, 1274–1276. [CrossRef]
47. Zhao, L.; Tang, D.; Cheng, T.; Tam, H.; Lu, C. Bound states of dispersion-managed solitons in a fibre laser at near zero dispersion. *Appl. Opt.* **2007**, *46*, 4768–4773. [CrossRef] [PubMed]
48. Lin, J.-H.; Chan, C.-W.; Lee, H.-Y.; Chen, Y.-H. Bound states of dispersion-managed solitons from single-mode Yb-doped fibre laser at net-normal dispersion. *IEEE Photonics J.* **2015**, *7*, 1–9.
49. Lu, B.L.; Wang, Y.; Qi, X.Y.; Chen, H.W.; Jiang, M.; Hou, L.; Huang, K.X.; Kang, J.; Bai, J.T. Observation of bound state solitons in tunable all-polarization-maintaining Yb-doped fibre laser. *Laser Phys.* **2017**, *27*, 075102. [CrossRef]
50. Zhao, L.; Tang, D.; Zhang, H.; Wu, X. Bound states of vector dissipative solitons. *IEEE Photonics J.* **2015**, *7*, 1–8. [CrossRef]
51. Li, L.; Ruan, Q.J.; Yang, R.H.; Zhao, L.M.; Luo, Z.Q. Bidirectional operation of 100 fs bound solitons in an ultra-compact mode-locked fibre laser. *Opt. Express* **2016**, *24*, 21020–21026. [CrossRef] [PubMed]

52. Luo, C.-J.; Wang, S.-M.; Lai, Y. Bound soliton fibre laser mode-locking without saturable absorption effect. *IEEE Photonics J.* **2016**, *8*, 1–9.
53. Wang, Z.Q.; Zhan, L.; Majeed, A.; Zou, Z.X. Harmonic mode locking of bound solitons. *Opt. Lett.* **2015**, *40*, 1065–1068. [CrossRef] [PubMed]
54. Gao, B.; Huo, J.; Wu, G.; Tian, X. Soliton molecules in a fibre laser mode-locked by a graphene-based saturable absorber. *Laser Phys.* **2015**, *25*, 075103. [CrossRef]
55. Liu, H.H.; Chow, K.K. High Fundamental-Repetition-Rate Bound Solitons in Carbon Nanotube-Based Fibre Lasers. *IEEE Photonics Technol. Lett.* **2015**, *27*, 867–870. [CrossRef]
56. Song, Y.F.; Zhang, H.; Zhao, L.M.; Shen, D.Y.; Tang, D.Y. Coexistence and interaction of vector and bound vector solitons in a dispersion-managed fibre laser mode locked by graphene. *Opt. Express* **2016**, *24*, 1814–1822. [CrossRef] [PubMed]
57. Al Khawaja, U. Stability and dynamics of two-soliton molecules. *Phys. Rev. E* **2010**, *81*, 056603. [CrossRef] [PubMed]
58. Afanasjev, V.V.; Akhmediev, N. Soliton interaction and bound states in amplified-damped fibre systems. *Opt. Lett.* **1995**, *20*, 1970–1972. [CrossRef] [PubMed]
59. Akhmediev, N.; Ankiewicz, A.; Soto-Crespo, J. Stable soliton pairs in optical transmission lines and fibre lasers. *J. Opt. Soc. Am. B Opt. Phys.* **1998**, *15*, 515–523. [CrossRef]
60. Bahloul, F.; Salhi, M.; Guesmi, K.; Sanchez, F.; Attia, R. Numerical demonstration of generation of bound solitons in figure of eight microstructured fibre laser in normal dispersion regime. *Opt. Commun.* **2013**, *311*, 282–287. [CrossRef]
61. Liu, X. Dynamic evolution of temporal dissipative-soliton molecules in large normal path-averaged dispersion fibre lasers. *Phys. Rev. A* **2010**, *82*, 063834. [CrossRef]
62. Agrawal, G.P. *Nonlinear Fibre Optics*, 4th ed.; Academic Press: Boston, MA, USA, 2007; pp. 153–154. ISBN 13 978-0-12-369516-1.
63. Komarov, A.; Amrani, F.; Dmitriev, A.; Komarov, K.; Meshcheriakov, D.; Sanchez, F. Dispersive-wave mechanism of interaction between ultrashort pulses in passive mode-locked fibre lasers. *Phys. Rev. A* **2012**, *85*, 013802. [CrossRef]
64. Soto-Crespo, J.; Akhmediev, N. Multisoliton regime of pulse generation by lasers passively mode locked with a slow saturable absorber. *J. Opt. Soc. Am. B Opt. Phys.* **1999**, *16*, 674–677. [CrossRef]
65. Cundiff, S.; Collings, B.; Knox, W. Polarization locking in an isotropic, modelocked soliton Er/Yb fibre laser. *Opt. Express* **1997**, *1*, 12–21. [CrossRef] [PubMed]
66. Grudinin, A.; Gray, S. Passive harmonic mode locking in soliton fibre lasers. *J. Opt. Soc. Am. B Opt. Phys.* **1997**, *14*, 144–154. [CrossRef]
67. Soto-Crespo, J.; Akhmediev, N.; Grelu, P.; Belhache, F. Quantized separations of phase-locked soliton pairs in fibre lasers. *Opt. Lett.* **2003**, *28*, 1757–1759. [CrossRef] [PubMed]
68. Weill, R.; Bekker, A.; Smulakovsky, V.; Fischer, B.; Gat, O. Spectral sidebands and multipulse formation in passively mode-locked lasers. *Phys. Rev. A* **2011**, *83*, 043831. [CrossRef]
69. Pilipetskii, A.; Golovchenko, E.; Menyuk, C. Acoustic effect in passively mode-locked fibre ring lasers. *Opt. Lett.* **1995**, *20*, 907–909. [CrossRef] [PubMed]
70. Kutz, J.; Collings, B.; Bergman, K.; Knox, W. Stabilized pulse spacing in soliton lasers due to gain depletion and recovery. *IEEE J. Quantum Electron.* **1998**, *34*, 1749–1757. [CrossRef]
71. Zaviyalov, A.; Grelu, P.; Lederer, F. Impact of slow gain dynamics on soliton molecules in mode-locked fibre lasers. *Opt. Lett.* **2012**, *37*, 175–177. [CrossRef] [PubMed]
72. Kagi, N.; Oyobe, A.; Nakamura, K. Temperature dependence of the gain in erbium-doped fibres. *J. Lightw. Technol.* **1991**, *9*, 261–265. [CrossRef]
73. Bolshtyansky, M.; Wysocki, P.; Conti, N. Model of temperature dependence for gain shape of erbium-doped fibre amplifier. *J. Lightw. Technol.* **2000**, *18*, 1533–1540. [CrossRef]
74. Nicolis, G.; Prigogine, I. *Self-Organization in Nonequilibrium Systems: From Dissipative Structures to Order through Fluctuations*; Wiley: New York, NY, USA, 1977; ISBN 13 978-0471024019.
75. Gumenyuk, R.; Okhotnikov, O.G. Impact of gain medium dispersion on stability of soliton bound states in fibre laser. *IEEE Photonics Technol. Lett.* **2013**, *25*, 133–135. [CrossRef]
76. Luo, Y.; Cheng, J.; Liu, B.; Sun, Q.; Li, L.; Fu, S.; Tang, D.; Zhao, L.; Liu, D. Group-velocity-locked vector soliton molecules in fibre lasers. *Sci. Rep.* **2017**, *7*, 2369. [CrossRef] [PubMed]

77. Komarov, A.; Sanchez, F. Structural dissipative solitons in passive mode-locked fibre lasers. *Phys. Rev. E* **2008**, *77*, 066201. [CrossRef] [PubMed]
78. Komarov, A.; Haboucha, A.; Sanchez, F. Ultrahigh-repetition-rate bound-soliton harmonic passive mode-locked fibre lasers. *Opt. Lett.* **2008**, *33*, 2254–2256. [CrossRef] [PubMed]
79. Olivier, M.; Roy, V.; Piché, M. Influence of the Raman effect on bound states of dissipative solitons. *Opt. Express* **2006**, *14*, 9728–9742. [CrossRef] [PubMed]
80. Dianov, E.; Luchnikov, A.; Pilipetskii, A.; Prokhorov, A. Long-range interaction of picosecond solitons through excitation of acoustic waves in optical fibres. *Appl. Phys. B Lasers Opt.* **1992**, *54*, 175–180. [CrossRef]
81. Kelly, S.M.J. Characteristic sideband instability of periodically amplified average soliton. *Electron. Lett.* **1992**, *28*, 806. [CrossRef]
82. Gordon, J.P. Dispersive perturbations of solitons of the nonlinear Schrödinger equation. *J. Opt. Soc. Am. B Opt. Phys.* **1992**, *9*, 91–97. [CrossRef]
83. Grapinet, M.; Grelu, P. Vibrating soliton pairs in a mode-locked laser cavity. *Opt. Lett.* **2006**, *31*, 2115–2117. [CrossRef] [PubMed]
84. Soto-Crespo, J.M.; Grelu, P.; Akhmediev, N.; Devine, N. Soliton complexes in dissipative systems: Vibrating, shaking and mixed soliton pairs. *Phys. Rev. E* **2007**, *75*, 016613. [CrossRef] [PubMed]
85. Zaviyalov, A.; Iliew, R.; Egorov, O.; Lederer, F. Multi-soliton complexes in mode-locked fibre lasers. *Appl. Phys. B Lasers Opt.* **2011**, *104*, 513–521. [CrossRef]
86. Zavyalov, A.; Iliew, R.; Egorov, O.; Lederer, F. Dissipative soliton molecules with independently evolving or flipping phases in mode-locked fibre lasers. *Phys. Rev. A* **2009**, *80*, 043829. [CrossRef]
87. Gui, L.; Xiao, X.; Yang, C.; Yang, X.; Zhu, J.; Li, X.; Zhu, H. Observation of various bound solitons of a fibre laser with carbon nanotubes and graphene as saturable absorbers. In *Proceedings of Quantum Electronics Conference & Lasers and Electro-Optics (CLEO/IQEC/PACIFIC RIM), Sydney, NSW, Australia, 28 August–1 September 2011; IEEE: Piscataway, NJ, USA, 2011*; pp. 1397–1399.
88. Chouli, S.; Grelu, P. Rains of solitons in a fibre laser. *Opt. Express* **2009**, *17*, 11776–11781. [CrossRef] [PubMed]
89. Chouli, S.; Grelu, P. Soliton rains in a fibre laser: An experimental study. *Phys. Rev. A* **2010**, *81*, 063829. [CrossRef]
90. Niang, A.; Amrani, F.; Salhi, M.; Grelu, P.; Sanchez, F. Rains of solitons in a figure-of-eight passively mode-locked fibre laser. *Appl. Phys. B* **2014**, *116*, 771–775. [CrossRef]
91. Chong, A.; Renninger, W.H.; Wise, F.W. Properties of normal-dispersion femtosecond fibre lasers. *J. Opt. Soc. Am. B Opt. Phys.* **2008**, *25*, 140–148. [CrossRef]
92. Bao, C.; Xiao, X.; Yang, C. Soliton rains in a normal dispersion fibre laser with dual-filter. *Opt. Lett.* **2013**, *38*, 1875–1877. [CrossRef] [PubMed]
93. Renninger, W.H.; Chong, A.; Wise, F.W. Area theorem and energy quantization for dissipative optical solitons. *J. Opt. Soc. Am. B Opt. Phys.* **2010**, *27*, 1978–1982. [CrossRef] [PubMed]
94. Kovalsky, M.G.; Hnilo, A.A.; Tredicce, J.R. Extreme events in the Ti: Sapphire laser. *Opt. Lett.* **2011**, *36*, 4449–4451. [CrossRef] [PubMed]
95. Finot, C.; Hammani, K.; Fatome, J.; Dudley, J.M.; Millot, G. Selection of extreme events generated in Raman fibre amplifiers through spectral offset filtering. *IEEE J. Quantum Electron.* **2010**, *46*, 205–213. [CrossRef]
96. Hammani, K.; Finot, C. Experimental signatures of extreme optical fluctuations in lumped Raman fibre amplifiers. *Opt. Fibre Technol.* **2012**, *18*, 93–100. [CrossRef]
97. Hammani, K.; Finot, C.; Millot, G. Emergence of extreme events in fibre-based parametric processes driven by a partially incoherent pump wave. *Opt. Lett.* **2009**, *34*, 1138–1140. [CrossRef] [PubMed]
98. Soto-Crespo, J.; Grelu, P.; Akhmediev, N. Dissipative rogue waves: Extreme pulses generated by passively mode-locked lasers. *Phys. Rev. E* **2011**, *84*, 016604. [CrossRef] [PubMed]
99. Lecaplain, C.; Grelu, P.; Soto-Crespo, J.; Akhmediev, N. Dissipative rogue waves generated by chaotic pulse bunching in a mode-locked laser. *Phys. Rev. Lett.* **2012**, *108*, 233901. [CrossRef] [PubMed]
100. Lecaplain, C.; Grelu, P.; Soto-Crespo, J.; Akhmediev, N. Dissipative rogue wave generation in multiple-pulsing mode-locked fibre laser. *J. Opt.* **2013**, *15*, 064005. [CrossRef]
101. Lecaplain, C.; Grelu, P. Rogue waves among noiselike-pulse laser emission: An experimental investigation. *Phys. Rev. A* **2014**, *90*, 013805. [CrossRef]
102. Runge, A.F.; Aguergaray, C.; Broderick, N.G.; Erkintalo, M. Raman rogue waves in a partially mode-locked fibre laser. *Opt. Lett.* **2014**, *39*, 319–322. [CrossRef] [PubMed]

103. Liu, Z.; Zhang, S.; Wise, F.W. Rogue waves in a normal-dispersion fibre laser. *Opt. Lett.* **2015**, *40*, 1366–1369. [CrossRef] [PubMed]
104. Liu, M.; Cai, Z.-R.; Hu, S.; Luo, A.-P.; Zhao, C.-J.; Zhang, H.; Xu, W.-C.; Luo, Z.-C. Dissipative rogue waves induced by long-range chaotic multi-pulse interactions in a fibre laser with a topological insulator-deposited microfibre photonic device. *Opt. Lett.* **2015**, *40*, 4767–4770. [CrossRef] [PubMed]
105. Liu, M.; Luo, A.-P.; Xu, W.-C.; Luo, Z.-C. Dissipative rogue waves induced by soliton explosions in an ultrafast fibre laser. *Opt. Lett.* **2016**, *41*, 3912–3915. [CrossRef] [PubMed]
106. Peng, J.; Tarasov, N.; Sugavanam, S.; Churkin, D. Rogue waves generation via nonlinear soliton collision in multiple-soliton state of a mode-locked fibre laser. *Opt. Express* **2016**, *24*, 21256–21263. [CrossRef] [PubMed]
107. Wang, P.; Hu, D.K.; Zhao, K.J.; Jiao, L.Y.; Xiao, X.S.; Yang, C.X. Dissipative rogue waves among noise-like pulses in a Tm fibre laser mode locked by a monolayer MoS_2 saturable absorber. *IEEE J. Select. Topics Quantum Electron.* **2018**, *24*. [CrossRef]
108. Pottiez, O.; Grajales-Coutiño, R.; Ibarra-Escamilla, B.; Kuzin, E.A.; Hernández-García, J.C. Adjustable noiselike pulses from a figure-eight fibre laser. *Appl. Opt.* **2011**, *50*, E24–E31. [CrossRef]
109. Soto-Crespo, J.M.; Akhmediev, N.; Ankiewicz, A. Pulsating, creeping and erupting solitons in dissipative systems. *Phys. Rev. Lett.* **2000**, *85*, 2937. [CrossRef] [PubMed]
110. Cundiff, S.T.; Soto-Crespo, J.M.; Akhmediev, N. Experimental evidence for soliton explosions. *Phys. Rev. Lett.* **2002**, *88*, 59. [CrossRef] [PubMed]
111. Runge, A.F.; Broderick, N.G.; Erkintalo, M. Observation of soliton explosions in a passively mode-locked fibre laser. *Optica* **2015**, *2*, 36–39. [CrossRef]
112. Bao, C.; Chang, W.; Yang, C.; Akhmediev, N.; Cundiff, S.T. Observation of coexisting dissipative solitons in a mode-locked fibre laser. *Phys. Rev. Lett.* **2015**, *115*, 253903. [CrossRef] [PubMed]
113. Soto-Crespo, J.M.; Akhmediev, N. Composite solitons and two-pulse generation in passively mode-locked lasers modeled by the complex quintic Swift-Hohenberg equation. *Phys. Rev. E* **2002**, *66*, 066610. [CrossRef] [PubMed]